Title

HEAVY-ION LINEAR INDUCTION ACCELERATORS AS DRIVERS FOR INERTIAL FUSION POWER PLANTS

Author

Hovingh, J.

Publication Date

1986-12-01

Lawrence Berkeley Laboratory
UNIVERSITY OF CALIFORNIA

Accelerator & Fusion
Research Division

Submitted to Fusion Technology

Heavy-Ion Linear Induction Accelerators as Drivers for Inertial Fusion Power Plants

J. Hovingh, V.O. Brady, A. Faltens,
D. Keefe, and E.P. Lee

December 1986

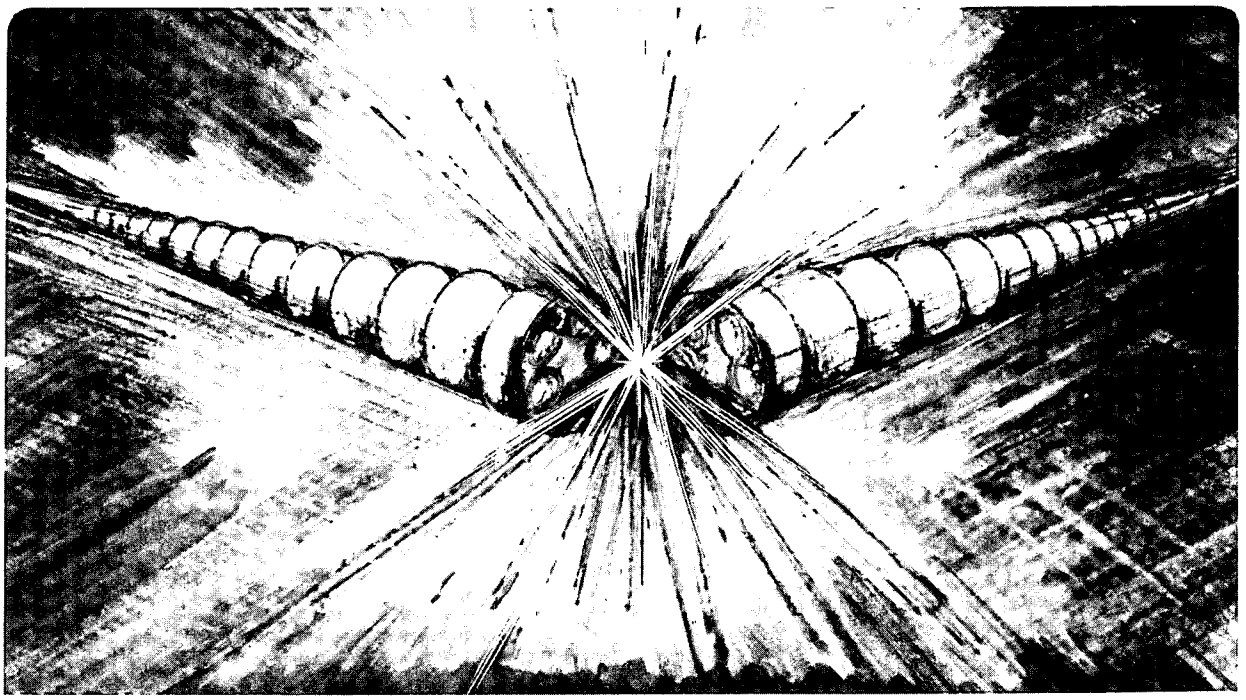

Prepared for the U.S. Department of Energy under Contract DE-AC03-76SF00098

DISCLAIMER

LBL-22757

HEAVY-ION LINEAR INDUCTION ACCELERATORS AS DRIVERS FOR INERTIAL FUSION POWER PLANTS*

J. Hovingh

Lawrence Livermore National Laboratory
University of California
Livermore, California 94550

V.O. Brady, A. Faltens, D. Keefe, and E.P. Lee

Lawrence Berkeley Laboratory
University of California
Berkeley, California 94720

December 1986

*This work was supported by the Office of Program Analysis, U.S. Department of Energy, under Contract No. DE-AC03-76SF00098.

HEAVY ION LINEAR INDUCTION ACCELERATORS AS DRIVERS FOR INERTIAL FUSION POWER PLANTS*

J. Hovingh

University of California

Lawrence Livermore National Laboratory

Livermore, CA 94550

V. O. Brady, A. Faltens, D. Keefe, and E. P. Lee

University of California

Lawrence Berkeley Laboratory

Berkeley, CA 94720

December 1986

List of Total Pages, Tables and Figures

---

*This work was supported by the Office of Program Analysis, U.S. Department of Energy, under Contract No. DE-AC03-76SF00098.

Heavy Ion Linear Induction Accelerators as Drivers for Inertial Fusion Power Plants

J. Hovingh

University of California, Lawrence Livermore National Laboratory, Livermore,CA 94550

V. O. Brady, A. Faltens, D. Keefe, and E. P. Lee

University of California, Lawrence Berkeley Laboratory, Berkeley, CA 94720

Abstract

A linear induction accelerator that produces a beam of energetic heavy ions (T ≈ 10 GeV, A ≈ 200 amu) is a prime candidate as a driver for an inertial fusion power plant. Some early perceptions were that heavy-ion driven fusion would not be cost competitive with other power sources because of the high cost of the accelerators. However, improved understanding of the physics of heavy ion transport and acceleration (supported by experimental results), combined with advances in accelerator technology have resulted in accelerator design costs about 50% of previous estimates. As a result, heavy-ion driven fusion power plants are now projected to be cost competitive with other conceptual fusion power plants. A brief formulation of transport and acceleration physics is presented here, along with a description of the induction linac cost optimization code LIACEP. Cost trends are presented and discussed, along with specific cost estimates for several accelerator designs matched to specific inertial fusion target yields. Finally, a cost-effective strategy using heavy ion induction linacs in a development scenario for inertial fusion is presented.

I. INTRODUCTION

The use of heavy ion accelerators as drivers to initiate inertially confined fusion reactions has been under study since 1975.[1,2] Early heavy ion accelerator concepts to provide the desired ion pulse (1 to 10 MJ of 5 to 20 GeV ions of atomic mass number between 130 and 238 amu) included an rf linac-accumulator system, a synchrotron-accumulator system, and an induction linac system.[2,3] Recent driver designs have concentrated on the rf linac-accumulator system for the HIBALL[4] and the HIBLIC-I[5] studies centered, respectively, in Germany and Japan. The Heavy Ion Fusion System Assessment (HIFSA) study in the USA adopts the induction linac, which does not require an accumulator because of the much more intense ion bunches that are accelerated. This paper describes the model computational tools and results of a cost-performance study of the induction linac portion of the HIFSA study. Also given is a strategy for reducing the buy-in cost of heavy ion fusion , proceeding from a single pulse test facility through an experimental power reactor using multiple pulses and exploiting the high pulse repetition capability of a linear accelerator.

An induction linac driver is now envisioned as a multiple beamlet transport lattice consisting of (N) closely packed parallel FODO transport channels. Each focussing channel is composed of a periodic system of focussing (F) and defocussing (D) quadrupole lenses with drift spaces (O) between successive lenses. Surrounding the transport structure are massive induction cores of ferromagnetic material and associated pulser circuitry which apply a succession of long duration, high voltage pulses to the N parallel beamlets. Longitudinal focussing is also achieved through the detailed timing and shape of the

accelerating waveforms (with feedback correction of errors). A multiple beam source of heavy ions operates at 2-3 MV, producing the net charge per pulse required to achieve the desired pellet gain. Initial current (and therefore initial pulse length) are determined by transport limits at low energy. The use of a large number of electrostatic quadrupole channels (N ~ 16 - 64) appears to be the least expensive focal option at low energies (below ~ 50 MV). This is followed by a lower number of superconducting magnetic channels (N ~ 4 - 16) for the rest of the accelerator. Merging of beams may therefore be required at this transition. Furthermore, some splitting of beams may be required after acceleration to stay within current limits in the final focus system.

The rationale for the use of multiple beams is that it increases the net charge which can be accelerated by a given cross section of core at a fixed accelerating gradient. Alternatively, a given amount of charge can be accelerated more rapidly with multiple beams since the pulse length is shortened and a core cross section of specified volt-seconds per meter flux swing can supply an increased gradient. However, an increase in the number of beamlets increases the cost and dimensions of the transport lattice and also increases the cost of the core for a given volt-sec product since a larger core volume is required. For a core of given cross section ($\propto$ volt-seconds/m), the volume of ferromagnetic material increases as its inside diameter is increased. Hence, there is a tradeoff between transport and acceleration costs with an optimum at some finite number of beamlets. The determination of this optimum configuration is a complex problem

depending on projected costs of magnets, core, insulators, energy storage, pulsers and fabrication.

The choice of superconducting magnets for the bulk of the linac is mandated by the requirement of system efficiency; this must be at least ~ 10% in an ICF driver and ideally $\gtrsim$ 20% to avoid large circulating power fractions (which result in a high cost of electricity (COE)). Induction cores are most likely to be constructed from thin laminations of amorphous iron, which is the preferred material due to its excellent electrical characteristics and flux swing. At a projected cost of ~ 8.8 $/kg (insulated and wound), this is a major cost item for the first 2-4 GV of a typical linac. At higher voltage, the cost of pulsers and fabrication of the high gradient column with insulators dominates.

Between the accelerator and the fusion reactor, the beamlets are separated radially in space and, if necessary, split with a kicker and magnetic septum. The drift lines leading to the final focus area are 200-600 m in length and used for ballistic compression as well as to match to the final focus configuration of the reactor. The transport lattice is composed of cold bore superconducting quadrupoles, bends, and possibly higher order elements needed to control momentum dispersion. As the beamlets compress, the transport of the high current becomes increasingly demanding, with the large apertures and the close packing of elements especially pronounced immediately before the final focus train.

The final focus system itself has parameters determined largely by the requirements of spot size on target, reactor size, and the handling of neutron, x-ray, and gas fluxes from the reactor. The final focus magnet train is composed of six or more magnetic quadrupoles of large

bore and several weak bends used to remove line of sight neutrons. Its total length is 50-100 m.

Transport within the reactor vessel has, in most studies, been assumed to take place in near vacuum ($P \lesssim 10^{-4}$ torr Li) to avoid disruption by the two-stream instability, or in a high pressure window ($P \sim 10^{-1}$ -10 torr), where the beam is also thought to be stable[6]. HIBALL specifies $P < 10^{-5}$ torr Pb vapor to avoid stripping of beam ions, which would lead to reduced target irradiance due to the beam's electric field. Unfortunately, several attractive reactor concepts (CASCADE,[7] HILIFE[8]) have residual gas pressures in the range 10^{-2} -10^{-3} torr Li at reasonable rep. rates; this pressure must be taken into account both for transport in the reactor and in maintaining vacuum in the final focus lines. Recent calculations[9] show that the two stream mode is benign at these pressures due to the detuning effects of beam convergence. The control of gas flux into the beamlines, and the process of stripping and neutralization in the reactor have not yet been examined in necessary detail, and are dealt with by plausible assumptions in the Heavy Ion Fusion System Assessment.

II. PHYSICS OF AN INDUCTION LINAC DRIVER SYSTEM

The driver system for an inertial fusion power plant featuring a linear induction accelerator is shown in Fig. 1. There are five main subsystems: the source/injector, a low voltage accelerator, a high voltage accelerator, the final beam compression/transport region between the accelerator and the reactor, and the final beam focussing magnet train. Each of these subsystems is subject to a set of physics constraints.

INDUCTION LINAC DRIVER (A=200, q=3)

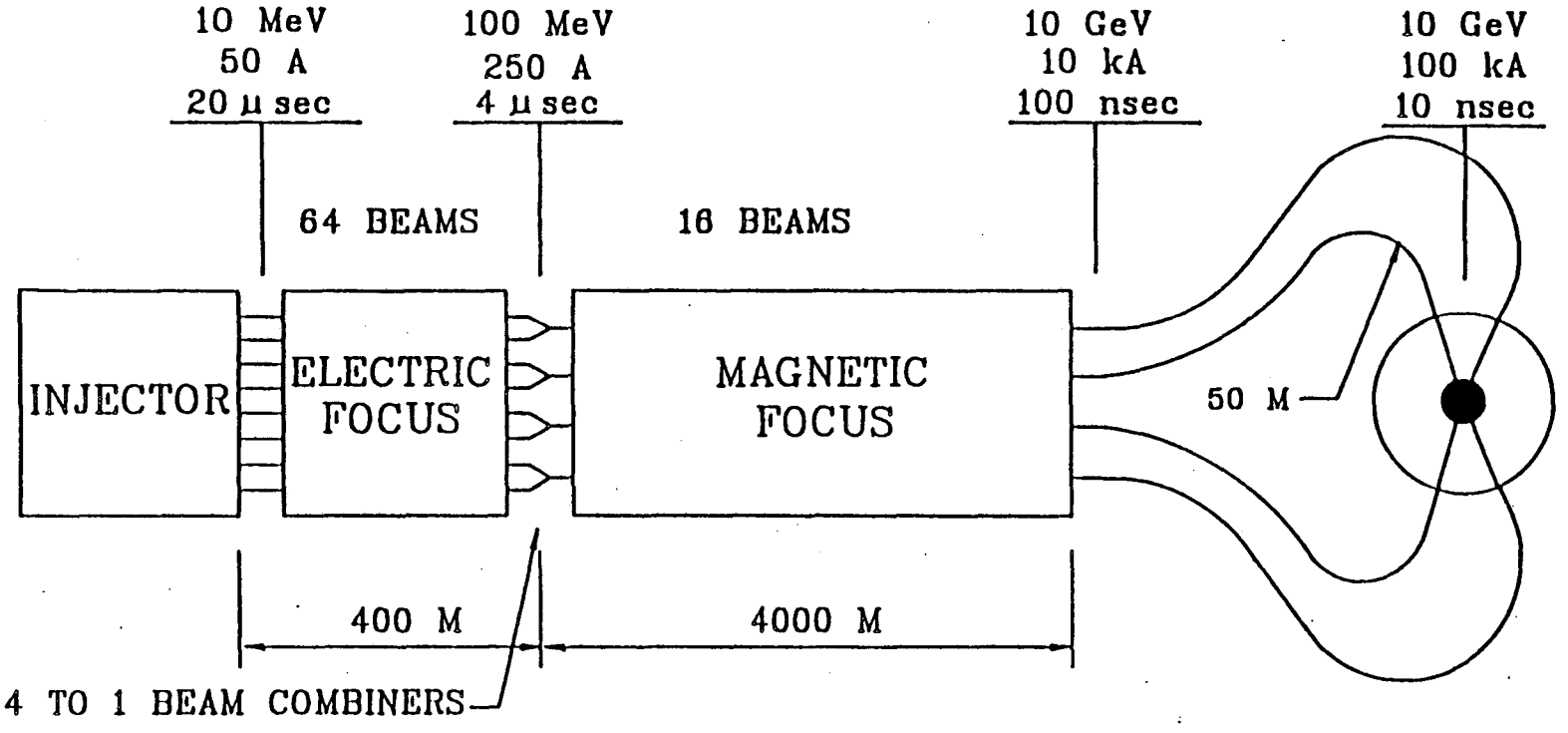

Fig. 1. Schematic of current concept for a 3.3 MJ driver that uses ions with A = 200, q = 3.

1. Source/Injector

The source produces the required quantity of ions in the desired charge state, and injects them into the low voltage section of the accelerator at a voltage which is high enough for efficient transport (~ 3 MV). The maximum current density available from a planar diode limited by space charge effects is given by the Child-Langmuir law:[10]

$$j = \frac{4\sqrt{2}}{9}\sqrt{\frac{e}{m_o c^2}\,\frac{\epsilon_o}{\mu_o}\,\frac{q}{A}}\;\frac{V_s^{3/2}}{d^2}$$

$$= 5.46 \times 10^{-8}\sqrt{\frac{q}{A}\,\frac{V_s^3}{d^4}} \quad A/m^2 , \qquad (1)$$

where V_s is the extractor voltage (typically $\approx$ 100 kV), d is the source extraction gap width, q is the ion charge state, and m_o is the atomic mass unit.

The normalized emittance ($\pi\epsilon_n$), which is the invariant transverse (x, x') phase volume occupied by a beamlet, is determined by the source characteristics and injector optics. For an ideal injector having no aberrations, the emittance can be simply related to the source radius (a_s) and temperature T_s according to

$$\epsilon_n \equiv 4\beta\gamma\left[\overline{x^2}\;\overline{x'^2} - (\overline{xx'})^2\right]^{1/2}$$

$$= 6.55 \times 10^{-5}\left(\frac{T_s}{A}\right)^{1/2} a_s \quad \text{m-r} , \qquad (2)$$

where T_s is given in eV.

From the basic equations (1) and (2), the source characteristics and some fundamental limits on the parameters of injected heavy ion beamlets can be inferred. Using large area diodes (~ 30 cm^2), heavy ion currents in the range of 1-2 amperes with $\epsilon_n \approx 10^{-6} - 10^{-7}$ m-r are plausible, although this capability has not yet been realized in practice. Currents of this magnitude are well matched to the low energy linac transport capability, while the emittance is 1-2 orders lower than the limit imposed by final focus. Hence, there is ample latitude for emittance growth during acceleration and the various beam manipulations.

2. Net Charge Per Pulse

After emerging from the sources, the ion beamlets are accelerated in a 2-3 MV high gradient column and injected into the linear induction accelerator. The total charge of the beamlets, Q, can be estimated from the fusion target requirements for specified final ion kinetic energy, T_o, and the total beam energy:

$$Q = qe \frac{W_o}{T_o} = \frac{W_o}{V_o} \qquad \text{Coulombs} \quad , \qquad (3)$$

where we use V = T/qe to denote the cumulative voltage. The length of the ion beamlets entering the low voltage portion of the accelerator is given by

$$\ell_b = \frac{Q}{N\lambda} \qquad \text{meters} \qquad (4)$$

where N is the number of parallel beamlets to be initially accelerated and λ is their line charge-density given in C/m. To avoid elongation of the initial bunch of charge as it leaves the injector, the beamlets are completely loaded into the accelerator before acceleration is begun. The subsequent acceleration rate must be gentle enough that the velocity tilt along the bunch length at a fixed point along the accelerator is

limited by

$$\frac{\delta v}{v} < 0.2 \qquad (5)$$

This requirement is imposed to prevent serious mismatch oscillations of the beamlets in the focal system.[11] The velocity tilt constraint is usually important only in the low voltage region of the accelerator.

3. Transport

In the absence of focussing, space charge and emittance effects would cause the ion beam to expand radially. To control the transverse motion of the ions, lenses are used along the length of the driver and subsequent transport lines. For this study, these lenses, which are either electrostatic or magnetic quadrupoles, are arranged in a FODO (focussing-drift-defocussing-drift) periodic lattice. A simple set of scale formulas relate the principal parameters of a magnetic FODO lattice [maximum beam radius (a), field at beam radius (B), and half period length (L)] to the principal beam parameters [electric current (I), normalized emittance (ϵ_n), and relativistic factor ($\beta\gamma$)]. It is also necessary to specify the fraction of the lattice occupied by quadrupoles (η), the phase advance per lattice period or tune (σ_0), and the depressed value of the tune (σ) resulting from the partial cancellation of the focal force by the beam's self generated field (see Fig. 2). These relations may be cast into the form[12]

$$B = \phi_1 (\sigma, \sigma_0, \eta) \left(\frac{q}{A}\right)^{1/2} (\beta\gamma)^{-5/2} I^{3/2} \epsilon_n^{-1} , \qquad (6)$$

$$a = \phi_2 (\sigma, \sigma_0, \eta) \left(\frac{q}{A}\right)^{-1/2} (\beta\gamma)^{1/2} I^{-1/2} \epsilon_n , \qquad (7)$$

$$L = \phi_3 (\sigma, \sigma_0, \eta) \left(\frac{A}{q}\right) (\beta\gamma)^2 I^{-1} \epsilon_n . \qquad (8)$$

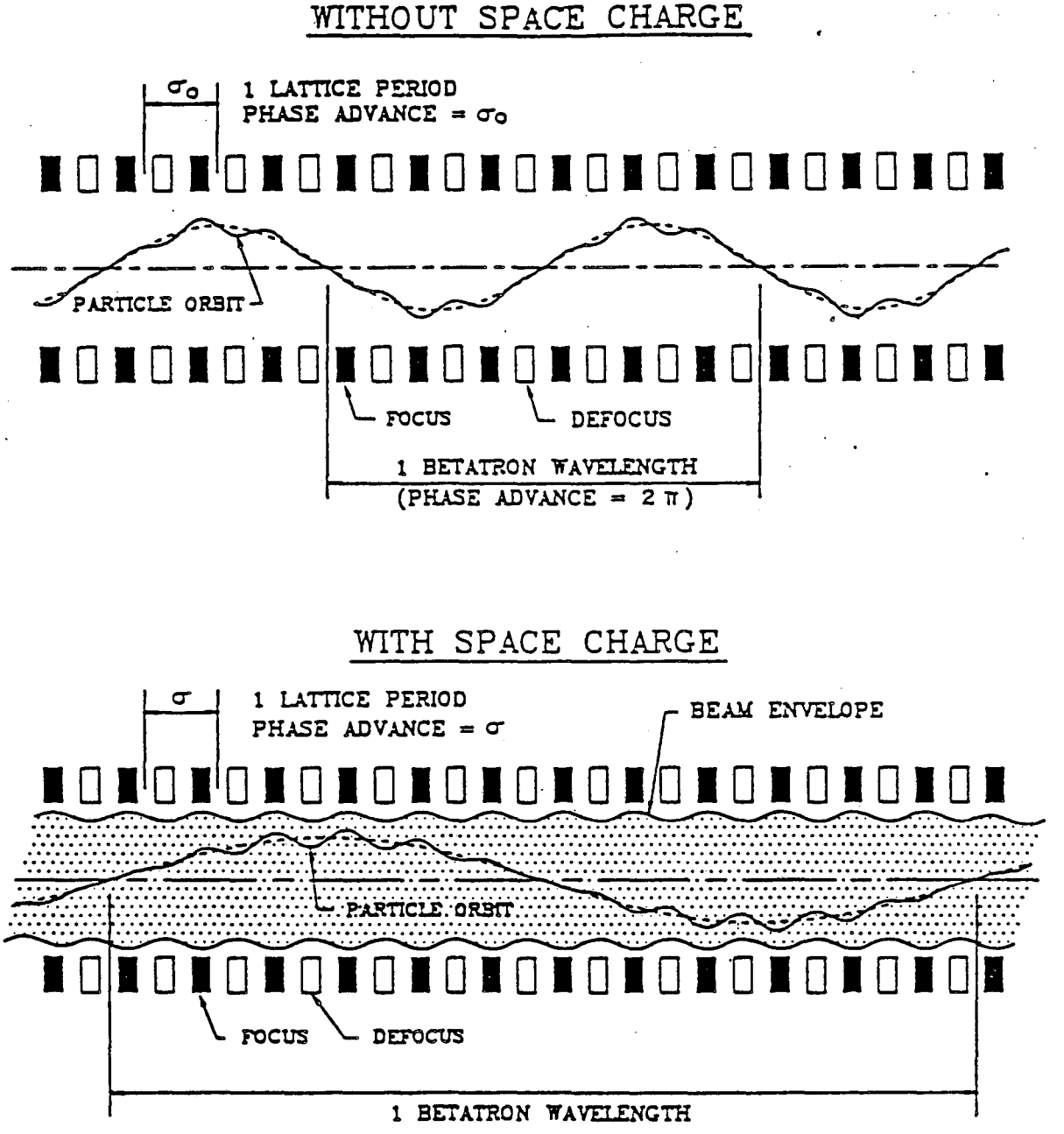

Fig. 2. Transverse motion of a particle in an alternating gradient focussing lattice. A lattice period corresponds to a focussing lens, a drift, a defocussing lens, and another drift (FODO). The definition of phase advance per period of the quasi-sinusoidal motion is shown for cases in which space-charge effects are negligible (top, σ_0), and strong (bottom, σ).

The relativistic factor is determined from the kinetic energy to be

$$\beta\gamma = \left[\left(\frac{T}{m_0Ac^2}\right)^2 + 2\left(\frac{T}{m_0Ac^2}\right)\right]^{1/2} \approx \left(\frac{2qeV}{m_0Ac^2}\right)^{1/2} . \qquad (9)$$

Here we have used the nonrelativistic approximation, which for the low velocities typically considered ($\beta \lesssim .3$) is in error by 1% or less. The functions $\phi_{1,2,3}$ have been determined by numerically solving the non-inear envelope equation for the matched beam radius in the given FODO Lattice.[13,14,15] For electrostatic quadrupoles, we must replace B in Eq. (7) with the ratio E/βc where E is the focussing electric field at the maximum beam radius.

The coeficients $\phi_{1,2,3}$ can be written in an analytic form[16] which is accurate to within a few percent when $\sigma_0 \lesssim 90°$, which is always the case due to considerations of stability. Both the analytical formulation and exact, tabulated results have been employed in the linac design code LIACEP, with very minor differences in results.

A less accurate approximation for the transport relations, developed by Maschke[17] using the continuous limit approximation for alternating gradient focussing, gives the transportable current, the mean beam radius ($\bar{a}$) and the lattice half period as[18]

$$I = (2.89\ MA)\left[1 - \left(\frac{\sigma}{\sigma_0}\right)^2\right]\left[\sigma_0^4\,(\beta\gamma)^5\,\eta^2\left(\frac{A}{q}\right)\left(\frac{\epsilon_n}{\sigma}\right)^2 B^2\right]^{1/3} , \qquad (10)$$

$$\bar{a} = (2.32\ m)\left[\left(\frac{\sigma_0}{\eta}\right)\left(\frac{1}{\beta\gamma}\right)\left(\frac{A}{q}\right)\left(\frac{\epsilon_n}{\sigma}\right)^2\left(\frac{1}{B}\right)\right]^{1/3} , \qquad (11)$$

$$L = (2.68\ m)\left[\left(\frac{\sigma_0}{\eta}\right)^2(\beta\gamma)\left(\frac{A}{q}\right)^2\left(\frac{\epsilon_n}{\sigma}\right)\left(\frac{1}{B}\right)^2\right]^{1/3} , \qquad (12)$$

where B given in Tesla, ϵ_n in meter-radians and the tunes in radians per period. From equations (10) and 11) the beamlet current density is

$$j = \left(.171 \frac{MA}{m^2}\right) \left[1 - \left(\frac{\sigma}{\sigma_0}\right)^2\right] \left[(\sigma_0)^2 \eta^4 (\beta\gamma)^7 \left(\frac{q}{A}\right) \left(\frac{\sigma}{\epsilon_n}\right)^2 B^4\right]^{1/3}. \qquad (13)$$

From Eq. (10), we anticipate that operation at low values of σ results in high values of transportable current I. However, this strategy also results in large values of the beam radius $\bar{a}$. In general, a cost minimum can be found, typically with σ in the range 8° – 24°, depending on the number of beamlets, total charge accelerated, emittance, and especially the ratio q/A.

4. Acceleration

The acceleration of the ion beam takes place in the drift section of the FODO lattice. The linear induction accelerator is equivalent to a transformer with the beam acting as a single turn secondary. A toroidal core of ferromagnetic material is excited by a primary winding from a high power pulser/modulator. Combining Faraday's Law with Stoke's Theorem, the change in the magnetic flux in the core is accompanied by an electric field across an acceleration gap

$$\oint E \cdot d\ell = -\int_S \frac{dB}{dt} \cdot dS \qquad (14)$$

where E is the electric field intensity, $d\ell$ is the elemental path length, B is the magnetic induction and dS is an elemental portion of the cross-section of the core. Since

$$\oint E \cdot d\ell = V_c \qquad (15)$$

where V_c is voltage applied to the core, equation (24) can be written as

$$\tau V_c = A(\Delta B) \qquad (16)$$

where A is the cross-sectional area of the core (the product of the core length and difference between the outer and inner core radii), ΔB is the magnetic flux swing in the core, and τ is the temporal duration of the pulse including the rise and fall time. The essential role of the core is to permit high voltage pulses of up to tens of microseconds duration (instead of nanoseconds) to be applied successively to the beam.

5. Transport to Reactor

Between the accelerator and the fusion reactor, the beamlets are separated and if necessary, split. The latter manipulation may be necessary in order to meet current transport limits at final focus or in the reactor. The drift lines leading to the final focus area consist of a sequence of bending and focussing magnets of total length 200-600 m. These are used for both ballistic compression and to match to the final focus configuration of the reactor. The transport lattice is composed of cold bore superconducting quadrupoles, bends, and possibly higher order elements needed to control the effects of momentum dispersion. As the beamlets compress, the transport of the high current becomes steadily more demanding, with the increasing apertures and the closer packing of elements becoming pronounced immediately before the final focus train of lenses.

At the end of acceleration, the ion pulse, is typically 100-400 ns in length, which is well matched to the band width of the pulse forming system. Subsequent reduction to the desired 5-20 ns length desired for the fusion pellet implosion dynamics is achieved by the mechanism of drift compression in the transport lines leading to the final focus

system. If the initial pulse length (in m) is ℓ_0 and the drift lines have length z_0, then a head to tail velocity tilt (at a fixed time) of approximately

$$\frac{\Delta v}{v} = \frac{\ell_0}{z_0}$$

must be applied in the final stages of acceleration. If, for example, ℓ_0=20 m and z_0 = 400 m, then the pulse tail must move 5% faster than the head in the transport lines. There are several important considerations in this approach.

(a) The bends in the transport system must handle the velocity tilt and space charge with a minimum of dispersive effects. There have been only rudimentary calculations of a design to do this.

(b) Longitudinal space charge forces reduce the velocity tilt as the pulse compresses; the initial tilt must be large enough that it is not entirely removed before the desired final pulse length is reached.

(c) Any residual tilt remaining in the pulse at the time of final focus will result in a severe second order chromatic aberration at the pellet. It is assumed that this can be compensated by the use of rapidly pulsed quadrupoles in an upstream location. That is, a time dependent envelope oscillation would be imposed which would cancel the time dependent aberration due to remaining tilt.

(d) The generation of longitudinal momentum spread by the inhomogeneous fields acting during compression is small (ideally $\Delta p/p < \pm 10^{-3}$). To date simulation of compression dynamics suggests only that the induced momentum spread can be on the order

of 10% of the initial tilt. This is larger than desired by a factor of several and may require special correcting elements.

6. Final Focus and Transport

The final focus system itself has parameters determined largely by the requirements of spot size on target, reactor size, and the neutron, x-ray, and gas fluxes from the reactor. The final focus triplets described by R. Martin[19] are well suited as the basic beam line components.

The minimum number of final beamlines (N_o) required to transport the beam ions to the fusion pellet with radius r can be estimated from a consideration of space charge effects in the reactor chamber. First consider that the beamlets traverse the chamber in vacuum and that space charge is the only defocussing effect. Then the beam envelope equation is

$$\frac{d^2a}{ds^2} = \frac{K_o}{a} \quad , \tag{17}$$

where K_o is the beamlet perveance:

$$K_o = \frac{2Iqe}{(\beta\gamma)^3 M_o c^3 A 4\pi\epsilon_o} \approx \frac{2Iq}{(\beta\gamma)^3 A\ (31 \times 10^6 \text{amp})} \quad . \tag{18}$$

The perveance is a dimensionless measure of beamlet current. The minimum beam radius resulting from Eq. (17) is

$$r = a_{lens} \exp(-\theta^2/2K_o) \quad , \tag{19}$$

where θ is the convergence cone half angle and

$$a_{lens} = L\theta \tag{20}$$

is the beam radius at the final lens. For a power reactor, we expect standoff length $L \approx 5$-10 m, $\theta = 10$-20 mr, and $r = 2$-4 mm. To make space charge negligible, we therefore require, in the absence of

neutralization

$$K_o \leq (.1)\ \theta^2 \qquad (21)$$

This condition leads to unacceptably large numbers of beamlets when the charge state exceeds $q \approx 2\text{-}3$, so some degree of neutralization must be invoked in general. The figure adopted in the HIFSA study is 90% neutralization, either from the ionization of residual gas or co-injection of electrons. Recent calculations by C. Olsen[6] indicate that the ion pulse is able to trap an electron cloud of sufficient density and low enough temperature to accomplish this. Thus we allow $K_o \leq \theta^2$. The number of beamlets N_o can be related to the total energy delivered to the pellet (W) by

$$N_o = \frac{W}{It_pT_o/qe} = \frac{4We^2q^2}{K_o(\beta\gamma)^5\ A\ m_o^2c^5 4\pi\epsilon_o t_p}$$

$$= (.138)\ \left(\frac{q}{A}\right)^2 \frac{W_{mJ}}{K_o(\beta\gamma)^5\ t_{ns}} \quad . \qquad (22)$$

where final pulse length is t_p (or t_{ns} in units of nanoseconds). For the typical case ($q = 3$, $A = 200$, $W_{mJ} = 4$, $t_{ns} = 10$, $K_o = 2.25 \times 10^{-4}$, $\beta\gamma = .33$), we get $N_o \geq 14.1$, which rounds up to $N_o = 16$ for symmetric two-sided illumination.

To produce a small radius (r) on the target, the normalized beamlet emittance (ϵ_n) must satisfy

$$\epsilon_n < \beta\gamma r\theta \qquad (23)$$

Allowance must also be made for the effect on spot size of momentum dispersion, various forms of jitter, and residual space-charge-induced blow up. A final focus system composed of quadrupoles and weak bends has dispersion at the target which leads in a practical design based on a pair of triplets to increased spot radius:

$$\Delta r \approx 8\, F\theta\, \frac{\Delta p}{p} \quad , \tag{24}$$

where F is the distance from pellet to the center of the final quadrupole. Without compensation by higher order elements, it is desirable to keep the momentum variations $\Delta p/p \lesssim 10^{-3}$. This is a severe requirement to be met by the accelerator system. Combining equations (21) and (22), the spot radius on target is

$$r = \sqrt{\left(\frac{\epsilon_n}{\beta\gamma\theta}\right)^2 + 64\left(F\theta\, \frac{\Delta p}{p}\right)^2} \tag{25}$$

Equations (1) through (25) constitute a brief summary of the physics foundation of drivers for inertial fusion based on linear induction accelerators. Further descriptions can be found in the literature.[20-26]

III. DESCRIPTION OF THE LINEAR INDUCTION ACCELERATOR

The linear induction accelerator portion of a heavy ion fusion driver consists of many subsystems. The transport system consists of the lens subsystem as well as the vacuum pumping subsystem. The acceleration system consists of the magnetic core subsystem as well as the modulator subsystem. Other major subsystems of the accelerator include the heat removal, beam alignment, control and diagnostics, insulation, supporting structure, and safety. A brief discussion of the major components follows.

The lens system consists of electrostatic or magnetic lens sets. In general, the lens configurations may include quadrupoles, sextupoles, higher order multipoles, and solenoids. Magnetic solenoids may, in principle, allow higher current densities per beam than quadrupoles at low ion kinetic energies, but are not under consideration for low energy transport at present due to a perceived economic disadvantage. At

moderate to high beam-voltages, the quadrupoles clearly allow a higher current density than the solenoids, and have been used in most conceptual driver designs. The selection of quadrupoles over higher order multipoles is based in part on the linearity of the quadrupole fields, which is desired in order to conserve emittance. The focussing quadrupoles can be either electrostatic, or magnetic. Due to the factor of velocity in the magnetic force law, magnetic quadrupoles are the choice of high energy and electrostatic quadrupoles at low energy. In a typical conceptual heavy ion fusion driver, the magnetic focussing system allows a higher beam current density than an electrostatic focussing system for voltages above some 10 to 100 MV. Several types of magnetic focussing quadrupoles can be used, for example, they can be either pulsed or steady devices. The pulsed quadrupoles and water cooled steady state electromagnets tend to be too inefficient for extensive use in a power plant. The steady state magnetic quadrupole transport system has an option of using either permanent and/or superconducting magnets. The achievable pole tip field strength for permanent magnets is, at the most, about 25% of that for superconducting magnets. Thus, from equation (13), the transportable current density through a permanent magnet quadrupole set is less than 16% of that using a superconducting magnet quadrupole set of comparable dimensions, and makes them unattractive for most scenarios.

The vacuum required in the beamline is determined by the allowable beam losses from interaction of the beam ions with the residual background gases. The stripping cross sections tend to decrease with the ion kinetic energy, so the vacuum requirement is more severe at the low voltage end of the accelerator. To keep the total beam losses from

interaction with the background gas to less than 5%, the background gas number density must be less than 10^7 - 10^9 particle/cm^3. These densities can be achieved in a well designed system using turbomolecular or cryogenic pumps.

The accelerator cores can be fabricated from either dielectric or ferromagnetic material. Since the ferromagnetic material has a higher electrical impedance to the driving source than a dielectric, the ferromagnetic cores are preferred. The cores are wound from thin tape, with insulation between the layers to allow for rapid field penetration and to decrease the eddy current loses, which ideally scale as the tape thickness squared divided by resistivity. Several cores can be driven in parallel, utilizing either radial or longitudinal stacking arrangements to increase the acceleration gap voltage.

The power delivered to the cores is increased from that delivered by the primary energy source by a series of pulse energy compression steps. A power supply charges a pulse generator such as a Marx generator or pulse forming network (which includes a high power switch). The output from this modulator drives the load current which is a parallel combination of the beam current (assumed constant during the pulse) and the core currents which increase during the pulse. A network consisting, for example, of a resistor and capacitor in series can be used to compensate for the increase in the core eddy current such that the total impedance of the core plus compensator is nearly constant.

This completes the description of some of the subsystems in a linear induction accelerator. In the next section we will describe the code LIACEP, which incorporates the described physics and subsystems, that is

used to optimize a heavy ion linear induction accelerator design to produce a minimum cost ICF driver.

IV. COST OPTIMIZATION CODE LIACEP

The Linear Induction Accelerator Cost Evaluation Program (LIACEP), developed at LBL, is an optimization program that varies several of the physical parameters of an induction linac in search of a minimum cost combination.[27,28] In addition to estimating the accelerator system cost and efficiency, LIACEP can be used to identify the components and materials that have a high leverage on the cost and efficiency of the accelerator system. These high leverage items are logical areas for research and technology development to reduce the system cost and increase the efficiency.

In using LIACEP, the ion mass and charge, the normalized transverse emittance, single particle and depressed tunes (betatron phase advance per period of the transport lattice), number of beamlets, charge per beamlet, and pulse repetition frequency are set. Also set are engineering parameters such as clearances, the acceleration module core material, and various limits to insulator voltages, module size, etc. Then, for a given particle kinetic energy, current and focussing system occupancy, the required field at the beamlet edge, the maximum beamlet envelope radius, and the half period of the transport lattice are determined using the approximation of Lee et al.[16] These quantities are used as input into a focussing system subroutine, which consists of a description of either electrostatic or superconducting quadrupoles. From the focussing system subroutine, the quadrupole length and the inner radius of the accelerator transport channel are obtained, as well as focussing system costs and power consumption that satisfy constraints

on the maximum pole tip field and beam radius and the minimum focussing system half period length to bore radius ratio. The acceleration system subroutines are then used to determine the accelerator module dimensions, power requirements, and costs for each module design. A cost comparison subroutine selects the minimum cost alternative of the various acceleration module designs. Successively higher values of current are then selected throughout a range limited by focal constraints; the minimum cost current is selected. Next, the ratio of the focussing system length to the half period length is increased and the calculations repeated. After the optimization at one particle kinetic energy point is completed, the process is repeated at a higher kinetic energy level. Finally, the total cost, length, power, efficiency, etc., (at the final kinetic energy T_o), are determined for this minimum cost accelerator system.

The module options investigated in the LIACEP are of three types.[28] The first type consists of cores external of the beam but internal to the insulator (see Fig. 3). The second type has the insulator external of the beam and internal to the cores. The third type is similar to the second type, but has an accelerator core wrapped around the focussing element. In most runs, the cost-optimized design option selects the third type of module in the low-to-medium voltage portion of the accelerator (< 1000 MV) and the second type of module in the high voltage region. The core material options in LIACEP include amorphous-iron, nickel-iron, silicon-iron, and ferrite. Amorphous-iron is usually the material of choice throughout the accelerator due to its superior combination of flux swing and response characteristics.

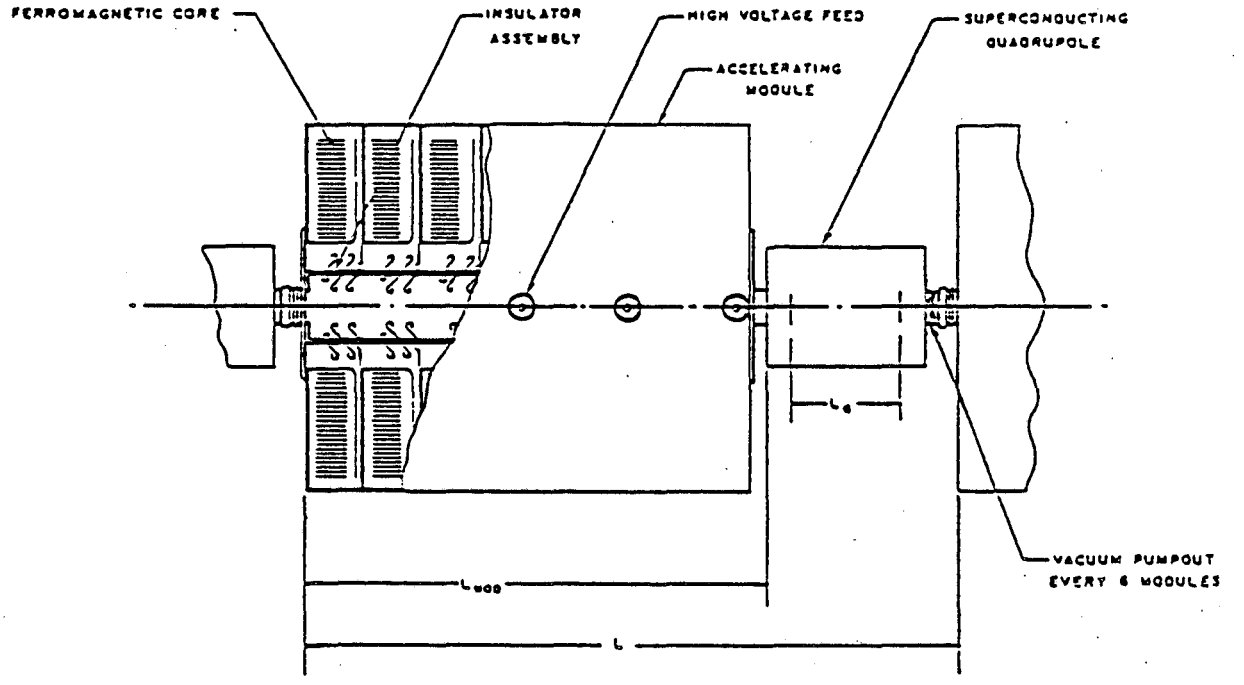

FERROMAGNETIC CORE MODULE - TYPE 2

Fig. 3. The accelerator core module features the insulator internal to the cores.

A. Cost Studies

Four cost studies were completed for HIFSA. The purpose of the first study was to examine the general features of LIACEP-generated designs, and to vary some of the physical parameters of an induction linac to examine their cost leverage. The purpose of the second study was to examine, throughout a large parameter space of ion, species, kinetic energies, emittances, beam total energies, pulse repetition frequencies, and number of beamlets, the minimized cost and the resultant efficiencies of an induction linac to be used in a variety of the HIFSA power plant systems. The third study was based on several possible power plant sizes, reactor chamber target yield capabilities, and target gain curves to identify the requirements on the linear induction accelerator driver, and using LIACEP, to determine the cost and efficiency of the drivers. The fourth study was performed to verify the modeling of the accelerator cost and efficiency for the various combinations of power plant subsystems for which the cost of electricity is a near minimum.

In all but the third study, the accelerator system assumes an initial cumulative voltage of 50 MV, so the LIACEP-generated costs do not include the low voltage (< 50 MV) portion of the accelerator, nor do they include the final compression, transport, and focussing portion of the system. These sections receive a separate treatment in the HIFSA study due to their distinctive roles and technologies. However, their costs are expected to be small compared to the accelerator (on the order of 20%). For the third study, the initial voltage of the accelerator was 3 MV, and magnetic focussing was used through the entire length of the accelerator.

B. Effects of Physical Parameters on Cost

A preliminary problem was run to determine the current state of LIACEP. This exercise reproduced the results presented in 1981 by Faltens et al.[29] for a 200 amu, unity charge state ion (Hg^+) using 4 beamlets of 75 μC of charge per beamlet and a total output energy of 3 MJ. The accelerator input voltage was 50 MV and the output voltage was 10 GV. The normalized transverse emittance was 1.17×10^{-5} meter-radians per beamlet and the tune was depressed from 60° to 24°. The acceleration cores were amorphous-iron, and the focussing was by superconducting quadrupoles. Finally, the pulse repetition frequency was 1 hertz, which is lower than typical values assumed for a fusion power plant (rep rate ≈ 3-10), resulting in a relatively low efficiency because the transport system's power requirement is independent of rep rate and at 1 Hz is ~ 50% of the total. Increasing the pulse repetition frequency increases substantially the accelerator system efficiency.

The Reference Case described above is used as a base for comparison with other runs with changes in some of the material properties assumed in the accelerator design. One such property is the vacuum insulator flashover gradient as a function of pulse duration, which has an appreciable effect on the system cost and efficiency. The assumed design limits for flashover gradient vary from more than 20 kV/cm for sub-microsecond pulses to 5 kV/cm for pulse lengths of 1 μs and longer. There are few, if any, 1 meter diameter, several meter long graded accelerating columns with several megavolts applied across them, let alone data on their time dependent flashover. Yet, it is permissible to examine the consequences of varying these limits. Increasing the short time flashover field by a factor of 2.5 will decrease the system cost by

13% and increase efficiency by 7.5%. Doubling the long pulse flashover field will reduce the cost by 14% and increase efficiency by 13%. Doing both will reduce cost by 24% and increase efficiency by 11%. Clearly, this provides motivation for investigation of the usable fields in a realistic structure and environment.

Increasing the breakdown voltage across vacuum gaps does not affect the cost of the accelerator system. This is due to the high cost of the insulator, which requires the insulator to be located between the acceleration core and the beam such that the regions between the acceleration cells in the module can be insulated. However, if the cost of the insulators can be reduced such that the core costs dominate at high cumulative voltage and the insulators may be placed outboard of the cores for a minimum cost acceleration module, then the breakdown voltage across vacuum gaps will become an important factor in the cost of the system.

The effect on the cost and efficiency of the accelerator system of the high voltage breakdown of ceramic insulators in vacuum as a function of length was also investigated. The voltage-breakdown design curves that were used allow about 38% of the voltage hold-off properties of high-power microwave tubes presented by Staprans,[30] which is in turn about 80% of the voltage-breakdown gradient of porcelain. By using a design curve at 40% of the breakdown gradient for porcelain the cost of the accelerator can be decreased by about 11%, and the efficiency increased about 14%. Re-X, a General Electric castable insulator, has about 80% of the voltage breakdown gradient of porcelain, such that it lies on Staprans design curve. Faltens recommends operating Re-X or other insulators at about half the voltage breakdown gradient;[31] this

criterion clearly affects the cost of the accelerator system. In general, the performance of the insulators can be improved (at increased cost) by more frequent subdivisions using gradient rings. The cost of the Re-X insulators is expected to be substantially less than that of porcelain insulators, so there may be a cost advantage to using them in the accelerator system despite their somewhat low performance.

To date we have identified the surface vacuum flashover gradient as a function of pulse duration for short pulses as a potential high-leverage field of research for induction linacs to be used as inertial fusion drivers. An experimental program that identifies the variables that affect short pulse flashover and determines the effects of 10^8 pulses on flashover would be a very cost-effective investment.

In addition, further studies on voltage breakdown as a function of length for ceramic insulators in vacuum may be cost-effective. Of special interest is the effect of size and configuration on the breakdown.

Using the reference case, but with the pulse repetition frequency increased to 5 hertz, the driver cost was examined as a function of beam energy, where the beam energy was varied by varying the beam charge and holding the final voltage at 10 GV. The cost was found to vary as a constant plus a linear term with energy. An increase in energy from 1 to 10 MJ results in an increase in cost by a factor of 3.3. For an output beam energy of 3 MJ, the cost varied as a constant plus a small term linear with the pulse repetition frequency. For an increase in frequency from 1 to 10 hertz, the cost increased by only 8 percent. For the reference case at 5 hertz the number of beamlets was varied between 1 and 16, with the minimum cost of 8 beamlets only 3.5% less than the cost of 4 beamlets.

V. HEAVY ION FUSION SYSTEMS ASSESSMENT PROJECT

A. Accelerator Cost Study

The Heavy Ion Fusion Systems Assessment (HIFSA) Project, sponsored by the DOE and EPRI, investigated the economic aspects of potential heavy-ion driven ICF power plants over a large parameter space.[32] To facilitate this, LIACEP was used to perform the cost and efficiency studies for an induction linac. The accelerator parameter space investigated for this study is given in Table I. The selection of a tune of 60° and depressed tune of 24° is conservative, as somewhat larger undepressed tunes and much smaller depressed tunes have been demonstrated to allow stable beam propagation in the laboratory in small scale experiments. The amorphous iron cores were selected because they were calculated to cost only about 67% of the silicon iron cores, and less than half of the nickel iron cores, and will operate at an efficiency of greater than 1.5 times that of the other core materials.

Qualitatively, the results for the parameter space investigated for the Heavy Ion Fusion Systems Assessment Project show that the rate of increase in accelerator cost with total beam energy increases is larger for low kinetic energy ions on target than for higher kinetic energy ions of the same mass, provide the number of beamlets is fixed. The number of beamlets that produces the minimum integrated cost of an accelerator increases with a decrease in the ion kinetic energy, as well as with an increase in the total beam energy. For a given voltage and total accelerator output energy, the optimum number of beamlets increases with a decrease in the ion charge to mass ratio and increases with an increase in the ratio of the depressed tune to the normalized emittance. At a given total beam energy and ion kinetic energy, the

Table I. Accelerator Parameter Space Investigated for Heavy Ion Fusion System Assessment

Ion Mass	130, 160, 190, 210 amu
Ion Kinetic Energy	5, 10, 15, 20 GeV
Beam Energy	1, 2, 3, 5, 10 MJ
Emittance (un-normalized)	1.5×10^{-5}, 3×10^{-5} m-radians
Pulse Repetition Frequency	5, 10, 15, 20 hertz
Number of Beamlets	4, 8, 16
Ion Charge State	+1
Tune : 60°, Depressed Tune : 24°*	
Initial Ion Kinetic Energy	50 MeV
Focussing System: Superconducting Quadrupoles	
Core Material: Amorphous Iron	

*Recent experiments show that depressed tune of 8° can be achieved; this will lead to cost savings.

accelerator cost increases with the ion mass for a fixed ion charge state. The cost of the accelerator decreases with an increase in emittance for a fixed depressed tune, over the parameter space investigated. However, for the given accelerator parameters (total output beam energy and ion kinetic energy), the cost of the accelerator is a function of ion charge to mass ratio as well as the depressed tune to normalized emittance ratio. Finally, the accelerator efficiency is related to the cost of the accelerator in that, in general, the highest efficiency accelerators tend to have the lowest optimized cost; moreover, efficiency can be increased by higher cost tradeoffs about the cost optimized designs, if necessary.

B. Accelerator Cost Study Based on Target Performance and Fusion Power

This portion of the accelerator study was based on the ICF reactor constraints and fusion power. Monsler et al. have identified the yield constraints on several generic reactor concepts.[33] The cost of a power plant is dependent on the fusion power output. This study was based on fusion powers of 1500, 3000, and 6000 MW_f and target yields of 300, 600, and 1200 MJ, which cover several generic types of reactor chambers. The pulse repetition frequencies of the accelerator system can be determined from the target yield and fusion power.

The required accelerator output parameters for a given target yield can be determined for a single shell target design using the Lindl-Mark gain curves.[34] These include the total energy and, for a given ion species, the emittance and ion kinetic energy. For a given target yield, the output energy, W, is determined based on the upper bound of the Lindl-Mark "best estimate" gain curve. Also determined is the $r^{3/2}R$ parameter where R is the range of the ions in g/cm^2 in the target

material and r is the target spot radius which must satisfy

$$0.1\ W^{1/3} < r < 0.2\ W^{1/3}\ (W, MJ;\ r, cm) \quad . \tag{26}$$

From the $r^{3/2}R$ parameter and the target spot radius, the desired range can be determined. From this range, the required ion kinetic energy can be specified from the ion range-energy curves of Bangerter et al.[35] From the ion kinetic energy and spot radius, for a given half angle of convergence (θ), the maximum normalized emittance of the accelerator beamlets can be determined assuming that it dominates the spot radius. This completes the description of the required accelerator output. Associated with the target gain and beam energy is a peak power requirement which can be independently modulated by the final transport drift lines.

For an ion mass of 200 amu, the ion kinetic energy and normalized emittance (based on a half-angle of convergence in the chamber of θ = 0.015 radians with no aberrations) as a function of target yield or accelerator output energy are shown in Fig. 4 for the upper, middle, and lower bounds on the spot radius for which high confidence exists in the gain curves. For a given value of $r^{3/2}R$, the range for the lower bound spot radius must be greater than for the upper bound spot radius. This requires, for a given ion mass, higher kinetic energies of the ions for the lower bound spot radius. The effect of the higher ion kinetic energy for the smaller spot radius is to require a smaller normalized transverse emittance than that for the larger spot radius.

The minimum cost of the accelerator system per unit fusion power as a function of target yield or accelerator output energy for the upper and lower bounds on the spot radius and several fusion powers is shown in Fig. 5. The cost of accelerators producing 3000 MW of fusion power

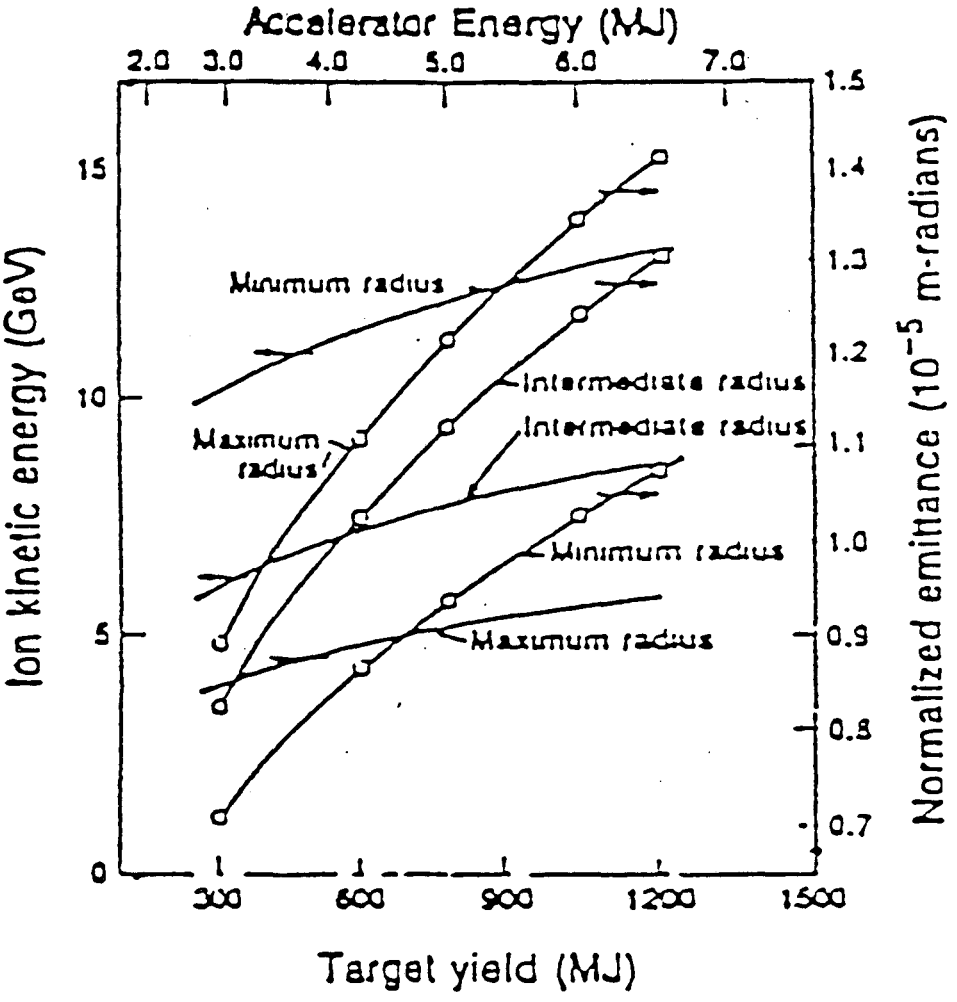

Fig. 4. Accelerator Parameter Space as a Function of Target Yield for a Range of Target Spot Radii for Ion Mass 200 amu.

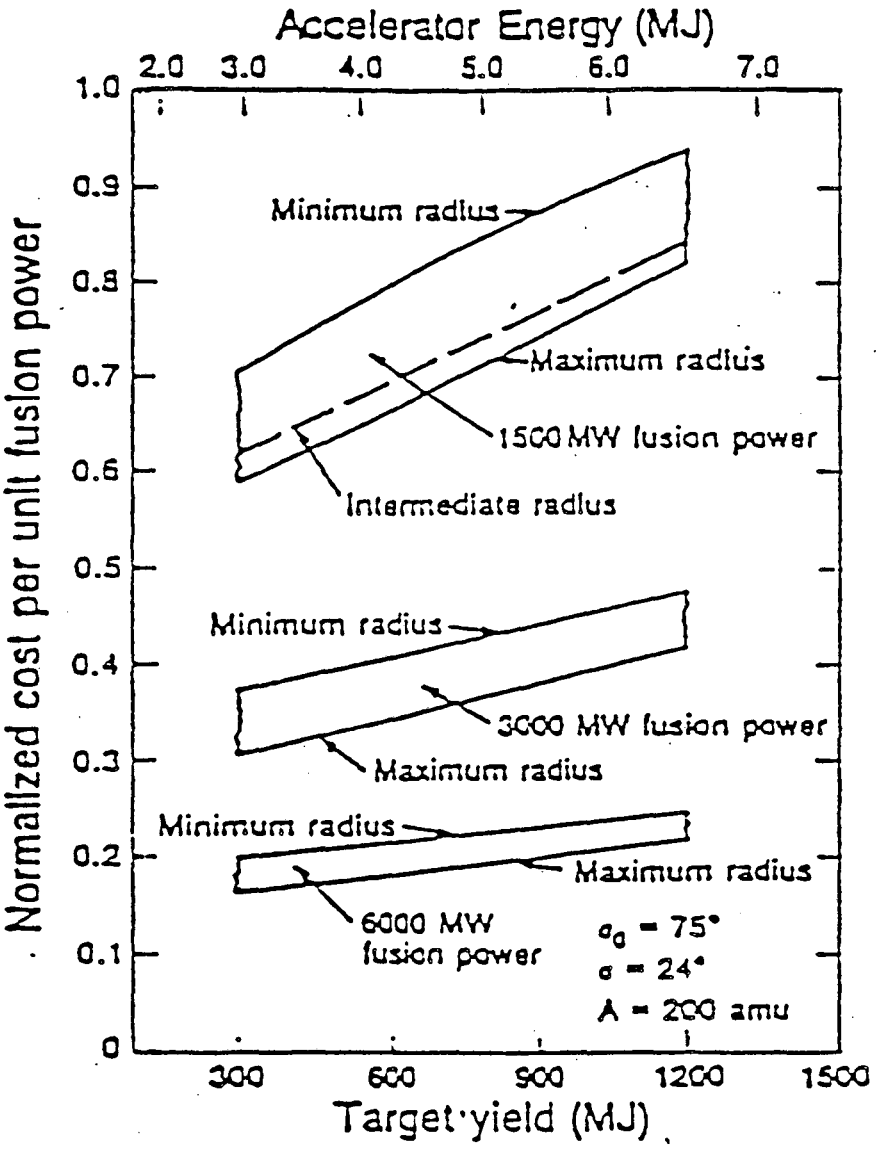

Fig. 5. Normalized Cost of Accelerator Per Unit Fusion Power as a Function of Target Yield for Several Fusion Power Outputs and a Range of Target Spot Radii for Ion Mass 200 amu, charge state +1.

Table II. Accelerator Output Characteristics, Efficiencies and 1979$ Costs for 300, 600, and 1200 MJ Target Yields and 3000 MW Fusion Power using 200 amu, q = +1 Ions.

ϕ = 0.5 MV/m; σ_0 = 75°, σ = 24°

Initial Voltage = 50 MV; Spot Radius = 0.1 $W^{1/3}$ cm

Range = R g/cm^2

Yield, MJ	300	600	1200
Pulse Rep. Rate, hertz	10	5	2.5
Energy, (W) MJ	2.91	4.25	6.57
Gain (G)	103	141	183
$r^{3/2}R$, 10^3 $cm^{-1/2}g$	7.2	10.4	15.9
Normalized Emittance (ε_n), μm-r	7.15	8.65	10.8
Ion Kinetic Energy, (E_i), GeV	10.12	11.46	13.24
Cost, G$			
Beamlets: 4	1.149	1.275	1.483
8	1.107	1.227	1.427
16	1.152	1.276	1.473
Efficiency, (η)%			
Beamlets: 4	21.2	21.5	21.6
8	22.7	24.6	26.2
16	20.7	23.0	25.3

at the lower bound spot size is given in Table II. The tune depression of the accelerator system is from 75° to 24°, and the normalized cost is based on the cost minimum of 4, 8, and 16 beamlets.[36] The cost for the lower bound spot radius is minimized at 8 beamlets, as given in Table II. The cost for the upper bound spot size is minimized at 16 beamlets. The cost for the intermediate spot radius shown for the 1500 MW_f case is also minimized at 16 beamlets.

For a given total energy, costs tend to vary inversely with the final ion kinetic energy due to the increased beam charge (for fixed normalized transverse emittance and tune depression). Thus, the cost for the maximum spot radius should be more than that for the minimum spot radius because a lower ion kinetic energy is associated with the maximum spot radius. The increased normalized emittance associated with the maximum spot radius tends to reduce the cost differential between the maximum and the minimum spot radius. However, the cost of acceleration of the lower ion kinetic energy (associated with the maximum radius) is more sensitive to the number of beamlets than that of the more energetic ions (associated with the minimum radius) for a fixed accelerator energy.

A final consideration of the analysis is the accelerator efficiency and ratio of fusion power to accelerator input power. For the minimum normalized cost shown in Fig. 5, the lowest accelerator efficiency is about 22% ranging to a maximum of about 32%. The ratio of fusion power to accelerator input power (ηG) ranges from 22 to 52. This ratio is substantially better than the minimum value of 10 and the desired value of 20 often quoted for inertial fusion.[33]

The costs given in Table II and shown in Fig. 5 can be reduced by increasing the charge state, increasing the undepressed tune, and decreasing the depressed tune limits. For example, the cost of the 4.25 MJ, 8 beamlet accelerator (above 50 MV) that produces 11.46 GeV ions can be reduced from 1.23 G$ to 0.639 G$ (1979$) by increasing the ion charge state to +3, increasing the undepressed tune to 85°, and decreasing the depressed tune to 10.5° while increasing the number of beamlets to 16. From perveance considerations, this accelerator system will require at least 16 beams focussed on target. The cost can be decreased further to 0.514 G$ by increasing the allowable vacuum surface flashover voltage gradient (ϕ) from 0.5 MV/m used above to 1.0 MV/m used in the Palaiseau Study[29]. The effect of these cost reduction techniques is to reduce the length of the accelerator (above 50 MV) from 10.7 to 2.23 km, and increase the efficiency from 24.6% to 34.5%. The somewhat longer front end (<50 MV) of the higher charge state option is more than offset by this large length reduction.

The cost of this accelerator can be further reduced from 0.514 to 0.483 G$ by double pulsing a 2.125 MJ accelerator. However, the efficiency decreases from 34.5% to 20.8% using current technology. Complete reactor plant system studies[37,38] have shown that the increased balance of plant costs due to the lower efficiency of double pulsing offsets the capital cost advantage of double pulsing.[39]

The increase in the charge state (q) of the ions may be facilitated by the development of the metal vapor vacuum arc (MEVVA) source which produces large quantities of ions in a range of charge states for most metals.[40] The higher charge state savings are due to the shortening of the accelerator, as discussed in this paper, with savings in the

quantity of cores and quadrupoles. Some of the cost savings may be used up by the increased number of beamlets in the final focus, which scales as q^2 in order to meet perveance constraints. These are discussed by Lee.[18,41] For the case selected for this paper, the number of beamlets determined from perveance considerations in the final focus does not exceed the number of beamlets in the accelerator.

The increase of the undepressed tune to 85° is speculative. However, there is some experimental evidence that this value of undepressed tune may be acceptable[18], as discussed later in this paper.

The use of a vacuum surface flashover voltage gradient of 1 MV/m results in the high acceleration gradients of about 2 MV/m in the final portion of the driver. These high acceleration gradients are adventurous, and are derived from the model used to estimate the enhancement of the flashover gradient at short pulse durations.

The use of multiple pulsing[42] to reduce the cost of the accelerator is most effective for ions with low kinetic energy. Cost savings of 30% can be realized with low kinetic energy (≈5 GeV) ions. A possible strategy for a low cost accelerator using low kinetic energy ions may be to use double pulsing coupled with a charge state of +2. This may ease the perveance conditions in the final focus and reduce the number of beamlets in the final focus to the target. Advances in switch tube technology may reduce the power consumption of the pulsers, which will increase the efficiency of the double pulsed accelerator.

Using the cost reduction strategy described above, three accelerators were analyzed using LIACEP to give target yields of 300, 600, and 1200 MJ using the minimum spot radius and the upper bound of the best estimate gain curve.[43] The fusion power, which is the product

of fusion yield and pulse repetition frequency, was fixed at 3000 MW. The charge state +3, 200 amu ions are injected into the accelerator with a kinetic energy of 9 MeV. This low voltage section of the accelerator consists of 64 beamlets, using superconducting quadrupoles and amorphous iron cores. The transition ion kinetic energy (qeV_c)for which it becomes cost effective to combine the 64 beamlets into 16 beamlets is the energy at which the total unit cost for the 64 beamlet system is equal to that of the 16 beamlet system. This transition ion energy is typically between 400 and 600 MeV for the cases considered. The 64 beamlets are then combined into 16 beamlets, and accelerated to the desired final kinetic energy. The accelerator output characteristics are as shown in Table II, and repeated in Table III.

The undepressed tune σ_o of 85° and the allowable vacuum surface flashover voltage gradient 1 MV/m are used for these accelerators. The depressed tune for each of the accelerators is given in Table III.

The costs and performance of the accelerators to produce target yields of 300, 600, and 1200 MJ are given in Table III for a fusion power of 3000 MW. The cost of the accelerator increases with the target yield, but the performance, measured as ηG (accelerator efficiency times target gain), also increases, resulting in a lower recirculating power fraction to the accelerator. The costs of the low voltage (<50 MV) section are about 20% of the main accelerator costs.

The unit costs (1979$) per volt for a driver which will produce a target yield of 300 MJ are shown in Fig. 6 as a function of the ion energy. At low ion energies, the core costs dominate the total cost. At high ion energies, the structure (including insulators) and pulsers are the more costly units. Integrating the costs over the ion kinetic

Table III. Accelerator Output Characteristics, Efficiencies and 1979 and 1985$ Costs for 300, 600, and 1200 MJ Target Yields and 3000 MW Fusion Power using 200 amu, q = +3 Ions.

ϕ = 1.0 MV/m; σ_o = 85°

Initial Voltage = 3 MV; Spot Radius = 0.1 X $W^{1/3}$ cm

Range = R g/cm^2; N = 16 beamlets, $V>V_c$

Yield, MJ	300	600	1200
Energy, (W) MJ	2.91	4.25	6.57
Gain (G)	103	141	183
$r^{3/2}R$, 10^3 $cm^{-1/2}g$	7.15	8.65	10.8
Normalized Emittance (ϵ_n), μm-rad	6.79	8.21	10.2
Ion Kinetic Energy, (E_i), GeV	10.12	11.46	13.24
Pulse Repetition Frequency, hertz	10	5	2.5
64 Beamlet Cost to 50 MV, M$ (1979)	108	124	162
64 to 16 beamlet transition voltage (V_c), MV	133	160	180
ϵ_n/σ, μm-rad/degree, $V<V_c$	1.1	0.82	1.1
Depressed Tune (σ), $V>V_c$, degrees	7.5	10.5	10.0
Total Cost, M$ (1979)	552	633	749
Total Cost, M$ (1985)	715	788	911
Total Length, km	1.97	2.22	2.57
Total Efficiency (η)%	26.9	28.7	29.0
ηG	27.7	40.5	53.1

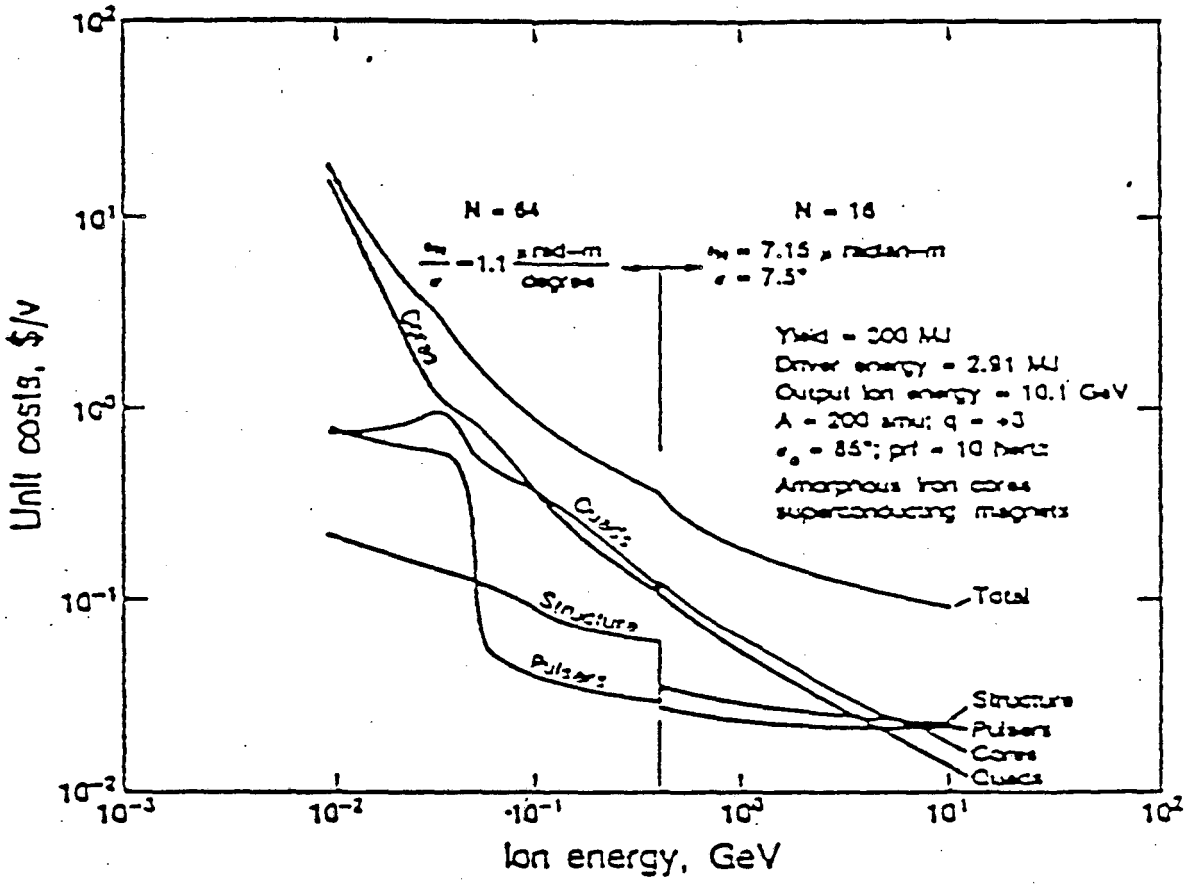

Fig. 6. Distribution of the accelerator costs (1979 dollars per volt) as a function of ion kinetic energy for a 300 MJ target yield producing a fusion power of 3000 MW. The transition ion energy for 64 beamlets to 16 beamlets is 400 MeV (133 MV). Above the transition ion energy the depressed tune is 7.5°.

energy gives the total costs for the complete accelerator. The cumulative distribution of the costs of the elements of this accelerator is shown in Fig. 7 as a function of the ion kinetic energy. The core costs are about 33% of the total cost of the accelerator. The superconducting magnet costs represent about 23% of the total costs of the accelerator. The structure (including insulators) and the pulsers represent about 17% and 15%, respectively, of the total costs. These cost percentages will change when the costs are updated to 1985, as discussed later in this paper.

The results for the low voltage section (<50 MV), as computed by LIACEP and shown in Fig. 6, are not very satisfactory. The cost differential between the 64 beamlet system and the 16 beamlet system is actually larger than currently calculated by LIACEP. This is due in part to not having a maximum velocity tilt ($\delta v/v$) limit in the code.[44] This limit on the tilt will increase the costs of the low voltage portion of the accelerator, where the beam length is long, by forcing a lower acceleration rate and increasing the cost of the quadrupoles. The effect of the tilt limit will be more severe with the smaller number of beamlets than with the larger number of beamlets. The costs of the pulsers shown in Fig. 5 can be reduced by driving several modules with a single pulser in the region where the ion kinetic energy is less than 60 MeV. This could reduce the pulser cost per volt by perhaps an order of magnitude in the low voltage (<20 MV) region. The LIACEP results show very low superconducting quadrupole fields in the low voltage section of the accelerator due to the constraint that their length to bore ratio must be greater than a minimum specified number. This constraint results in large beamlet diameters, with concomitant large quad and core costs. By relaxing this constraint, the depressed tune could be increased which would increase the quadrupole field and reduce the beamlet diameter, resulting in a reduction

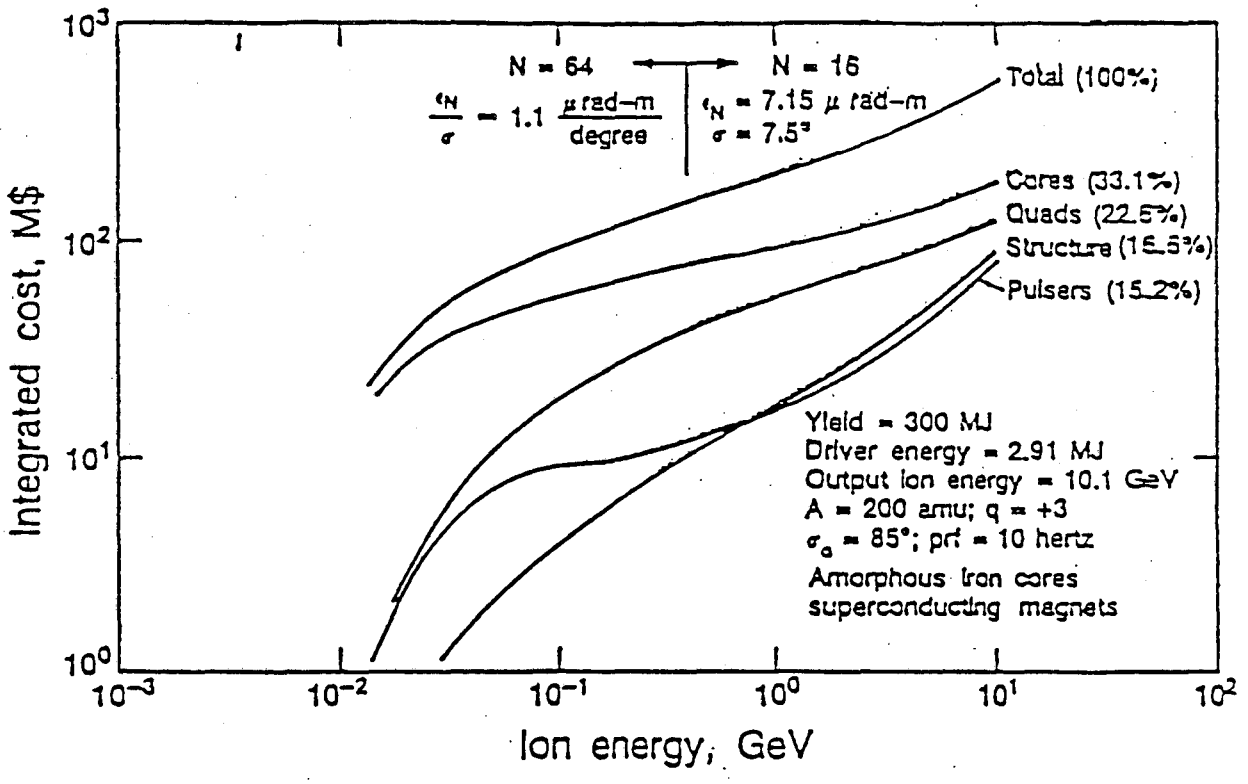

Fig. 7. Cumulative distribution of the accelerator costs (1979 dollars) as a function of ion kinetic energy for a 300 MJ target yield producing a fusion power of 3000 MW. The transition ion kinetic energy for 64 beamlets to 16 beamlets is 400 MeV.

in the quad and core costs.[44] Also, the use of electrostatic quadrupoles in the low voltage region should decrease the costs.

The combining of 64 beamlets into 16 beamlets in space and time may result in a cost savings. This combination of beamlets will result in an increased emittance in the region with the smaller number of beamlets (or conversely, require a reduced emittance in the region with the larger number of beamlets). Thus, there is a maximum number of beamlet combinations that can be allowed that will give the required spot size on target with a given source brightness. In addition, the depressed tune should be held proportional to the emittance. The output emittance is determined from target considerations, and the depressed tune in the high voltage portion of the accelerator is selected to minimize the cost of this portion of the accelerator. The decrease in emittance in the low voltage section due to the combining of beamlets will require a reduction in the depressed tune to minimize the cost in this section. There may be a lower limit to the depressed tune before instabilities occur that may offset some of the cost advantages of combining beamlets.

Additional cost savings can be made by changing the depressed tune along the length of the accelerator. For the case of the 4.25 MJ driver given in Table III, but with a vacuum surface flashover voltage gradient of 0.5 MV/m, with 16 beamlets and an initial ion energy of 150 MeV, the cost savings, by reducing the depressed tune from 10.5° to 8° for ion energies between 200 and 1500 MeV, was somewhat greater than 7 M$.

Three accelerators using mass 133, charge state +2 ions were also analyzed to give target yields of 300, 600, and 1200 MJ using the minimum spot radius and the upper bound of the best estimate gain curve.[45] The fusion power was fixed at 3000 MW. The ions are injected

into the accelerator with a kinetic energy of 6 MeV. The subsequent low voltage section of the accelerator consists of 64 beamlets, using superconducting quadrupoles and amorphous iron cores as before. The transition ion kinetic energy for which it becomes cost effective to combine the 64 beamlets into 16 beamlets is the energy at which the total unit costs for the 64 beamlet system is equal to the 16 beamlet system. This transition ion kinetic energy (qeV_c) is typically between 200 and 400 MeV for the 133 amu, charge state +2 ion cases considered. The 64 beamlets are then combined into 16 beamlets, and accelerated to the desired final kinetic energy. The accelerator output characteristics are as shown in Table IV.

The undepressed tune (σ_o) of 85° and the allowable vacuum surface flashover voltage gradient (ϕ) of 1 MV/m is used for these accelerators. The depressed tune for each of the accelerators is given in Table IV.

The costs and performance of the accelerators are given in Table IV. The cost of the accelerator increases with the target yield, but the performance, measured as ηG (accelerator efficiency times target gain), also increases, resulting in a lower recirculating power fraction to the accelerator.

The costs of the accelerators given in Tables II, III, and IV are for a mature technology in 1979 dollars and projected component costs. The cost estimate escalation factor for a typical major construction project at high energy physics laboratories with a cost distribution of 70% conventional construction and 30% technical components, from 1979 dollars to 1985 dollars, is 1.606. This cost escalation factor should not be applied across the board to the costs estimated by LIACEP for the following reasons.

Table IV. Accelerator Output Characteristics, Efficiencies and 1979 and 1985$ Costs for 300, 600, and 1200 MJ Target Yields and 3000 MW Fusion Power using 133 amu, q = +2 Ions.

ϕ = 1.0 MV/m; σ_o = 85°

Initial Voltage = 3 MV; Spot Radius = 0.1 X $W^{1/3}$ cm

Range = R g/cm^2; N = 16 beamlets, $V>V_c$

Yield, MJ	300	600	1200
Energy, (W) MJ	2.91	4.25	6.57
Gain (G)	103	141	183
$r^{3/2}R$, 10^3 $cm^{-1/2}g$	7.2	10.4	15.9
Normalized Emittance (ε_n), μm-rad	6.79	8.21	10.2
Ion Kinetic Energy, (E_i), GeV	6.077	6.885	7.953
Pulse Repetition Frequency, hertz	10	5	2.5
64 to 16 beamlet transition voltage (V_c), MV	110	150	200
ε_n/σ, μm-rad/degree, $V<V_c$	1.1	0.82	1.1
Depressed Tune (σ), $V>V_c$, degrees	7.1	10.1	9.5
Total Cost, M$ (1979)	545	635	757
Total Cost, M$ (1985)	706	775	913
Total Length, km	1.77	2.16	2.40
Total Efficiency (η)%	27.6	31.6	29.8
ηG	28.4	44.6	54.5

The amorphous iron cores, including both the material and fabrication, were priced at $8.81 per kilogram in 1979. These costs are still appropriate. The cost of the superconductor material and fabrication are the same in 1985 dollars on a per unit mass basis as they were in 1979 dollars, but the amount of cable required for a given field has decreased by about 25% due to improvements in cable configuration and manufacture, which have resulted in an increased critical current. The development of castable insulators has cut the cost of the brazed insulators in the structure by about an order of magnitude. The Superconducting Super Collider (SSC) cost estimates for tunneling of 4. K$/m in 1985 dollars is about the same as the accelerator building costs used in LIACEP (5.1 K$/m). However, the cost of stored energy has escalated from $2.80 per Joule to about $8.50 per Joule for long-lived capacitors.

A rough estimate of the escalation of the accelerator costs given in 1979 dollars to 1985 dollars is as follows:

$$
\begin{aligned}
\text{1985 cores} &\approx \text{1979 cores} \\
\text{1985 quads} &\approx \text{1979 quads} \\
\text{1985 pulsers} &\approx 3. \times (\text{1979 pulsers}) \\
\text{1985 structure} &\approx 0.5 \times (\text{1979 structure}) \\
\text{1985 remainder} &\approx 1.606 \times (\text{1979 remainder}).
\end{aligned}
$$

These escalation costs may be higher than if the appropriate costs were placed in LIACEP because the costing algorithms in LIACEP are quite complex. The superconducting quadrupole cost escalation factor of 1.0 given above takes into account that the quads consist of more than

superconductor. Likewise the cost escalation factor of 0.5 for the structure takes into account that the structure consists of more than insulator. The cost escalation factor of 3 for the pulsers does not take into consideration that the pulsers consist of more than energy storage, but does allow for a factor of 10 increase in repetition rate and total life.

The costs escalated to 1985$ of the accelerators using mass 200, charge state +3 ions and mass 133, charge state +2 ions are given in Tables III and IV respectively.

The distribution of the accelerator costs using mass number 133, charge state +2 ions is given in Table IV in both 1979$ and 1985$ for a driver that will produce a target yield of 300 MJ and a fusion power of 3000 MW. For the driver optimized to 1979$, the cores are the most expensive component, followed by the superconducting quadrupoles. Escalating this design to 1985$ results in the pulsers becoming the most expensive component, followed by the core. If the driver design is optimized to 1985$, the cost distribution and costs will differ from those shown in Table V.

The costs of the accelerators using 133 amu, charge state +2 ions are within 2% of those using 200 amu, charge state +3 ions for a given target yield. For all cases, the charge state to mass ratio was held constant. For a given target yield, the (depressed tune to normalized emittance) ratio was held constant. The difference in the cost and performance for a given target yield is due to the difference in the required ion kinetic energy (and hence, beam charge) of the two particle masses to satisfy the range requirement for the specified target yield.

Table V. Distribution of Accelerator Costs for a Driver Producing a Target Yield of 300 MJ and a Fusion Power of 3000 MW using 133 amu, q = +2 Ions.

Basis Year	1979	1985
Total Cost, M$	545	706
Core, %	34.2	26.5
Structure, %	15.2	5.9
Pulsers, %	14.9	34.4
Quads, %	23.6	18.3
Remainder, %	12.1	14.9

The 1985$ cost of the accelerator using 133 amu, charge state +2 ions optimized to 1979$ costs is cheaper than that using 200 amu, charge state +3 ions for low target yields. However, the final transport costs of the lower mass, lower charge state ions may be greater than the higher mass, higher charge state ions due to the increased number of beamlets on target required by the perveance limitation in the final focus.[18,46] The required number of beamlets on target is about 33% greater for the 133 amu, +2 ions than for the 200 amu, +3 ions due to the difference in the required ion kinetic energy of the two particle masses to satisfy the range requirement for the specified target yield. The number of beamlets for final transport of the 200 amu, +3 ions on target is matched to the 16 beamlets in the high voltage end of the accelerator such that no beam splitting is required for the final transport to the target. The 16 beamlets of the 133 amu, +2 ions from the high voltage end of the accelerator may need to be split into a minimum of 22 beamlets, with a decrease in the beamlet emittance in the accelerator to preserve the spot radius on target. The decrease in the emittance may require a lower depressed tune in the accelerator to mitigate the impact of the lower emittance on the accelerator costs. If the depressed tune is reduced too far, stability problems may occur in beamlet transport.[47] An additional consideration is that the emittance increases due to excessive combining and/or splitting of the beamlets can lead to an unacceptable loss of beam brightness at final focus.

The cost and performance of the accelerators to produce a given target yield using mass 133, charge state +2 ions is very close to that using mass 200, charge state +3 ions. The final focussing requirements

for the mass 133, charge state +2 are more demanding than those for the mass 200, charge state +3 ions. Beamlet splitting may be required to satisfy the final focussing requirements for the driver using the mass 133, charge state +2 ions.

VI. LIACEP ANALYSIS OF SELECTED HIFSA PROJECT CODE SAMPLE CASES

The inertial fusion power plant systems analysis code ICCOMO was written by McDonnell Douglas Astronautics Company for the HIFSA Project.[48] ICCOMO used curve fits to LIACEP calculations of the accelerator cost in 1979$ and performance for the parameter space given in Table I. The LIACEP results for ion charge state +1, an undepressed tune (σ_0) of 60°, depressed tune (σ) of 24° and a vacuum voltage flashover gradient (ϕ) of 0.5 MV/m used in ICCOMO were multiplied by "appropriate" factors to account for the higher charge state, undepressed tune, voltage flashover gradient and lower depressed tune presently believed to be feasible, and the conversion to 1985 dollars.

The cost and performance of the accelerators for three promising power plant systems were selected for verification by LIACEP of the curve fit and factors used in ICCOMO. The three cases represent a wide variation in the accelerator output energy and pulse repetition frequency. The output parameters of the accelerators for the three cases as well as their cost and performance are given in Table VI for the acceleration region above 50 MV. Three costs are given for each accelerator; the LIACEP-computed cost in 1979 dollars, the LIACEP computed cost converted to 1985 dollars, and the cost generated by ICCOMO. These new results, when put into ICCOMO, should reduce the cost of electricity of inertial fusion power plants corresponding to Cases 15 and 16 of Table VI.

Table VI. Comparison of LIACEP Results (V>50 MV) with those of ICCOMO for A=130 amu Ions.

Parameters	LIACEP	ICCOMO
σ_o (°)	85	60
σ (°)	8.5	24
ϕ (MV/m)	1.0	0.5
q	+3	+1
N beamlets	16	16

Case	#1	#15	#16
Frequency, hertz	11	3	5
Ion kinetic energy, GeV	7	8	7
Total Energy, MJ	4.72	7.76	3.40
Normalized Emittance, μm-radians	11.3	11.7	9.38
Cost, M$			
LIACEP (1979$)	500	570	380
LIACEP (1985$)	700	740	480
ICCOMO (1985$)	727	840	614
Efficiency, %			
LIACEP	39.5	38.2	36.2
ICCOMO	41.2	32.3	35.5
Length, km			
LIACEP	1.61	1.99	1.51
ICCOMO	1.39	1.68	1.31

A. Physical Basis for Cost Reduction Strategy

Heavy ion driver studies have for several years concentrated on the use of charge state q = 1 and the highest available mass (A ≈ 200), however, it has been noted that increased charge state may be desirable in order to lower linac cost and length[29]. It is clear that increased q or decreased A decreases the final cumulative acceleration potential required to reach a final given ion velocity, but it is less clear, given the constraints of transportable current and range in the target, that this is a useful path to take. Examination of Eqs. (6)-(9) shows that increased q and decreased A are equivalent as regards transport for given V. The differences are in the availability of good sources and range in the target at fixed final velocity.

For ion range in the target the situation is clear: at $\beta \approx .3$ an ion of mass number A = 100 has about twice the range as an ion of mass number 200. Other things being equal the doubled range would halve the specific energy deposition, and to achieve equal target gain the spot radius would need to be decreased approximately by a factor of $\sqrt{2}$.

The only heavy ion sources available at present which can be readily adapted to driver requirements are the contact ionization of Cesium and the Mercury vapor arc. However, the metal vapor vacuum arc (MEVVA),[40] which produces copious ions of high brightness in a range of charge states for all metals, is undergoing an impressive development and may be considered as a possible future driver source. The main problem in adaptation appears to be the removal of unwanted charge states from the pulse before introduction into the induction linac.

We assume here that the highest mass ions available from good sources will be used in a driver because of their short range, and that

charge state can be increased arbitrarily until some transport or focal limit is reached. If σ/σ_0 is small, so that the factor $[1-(\sigma/\sigma_0)^2]$ in Eq. (10) can be replaced by unity, then the following scale relations are found for $(\frac{q}{A})\rightarrow(\frac{q}{A})'$:

At each value of voltage V, comparing beams of the same normalized emittance (ϵ_n) but differing charge to mass ratios we have

$$(\frac{q}{A})\rightarrow(\frac{q}{A})' = \alpha\,(\frac{q}{A}) \ , \tag{27}$$

$$V \rightarrow V,\ a \rightarrow a,\ \eta B \rightarrow \eta B,\ \epsilon_n \rightarrow \epsilon_n,\ \sigma_0 \rightarrow \sigma_0 \ ,$$

$$I \rightarrow \alpha I,\ \tau_p \rightarrow \tau_p \ ,$$

$$E \rightarrow \alpha E,\ \beta\gamma \rightarrow \alpha^{+1/2}\,\beta\gamma \ ,$$

$$\sigma \rightarrow \alpha^{-3/4}\,\sigma,\ L \rightarrow \alpha^{-1/4}\,L \ ,$$

$$\text{volt-sec/m} \rightarrow \text{volt-sec/m} \ .$$

The significance of this transformation is that the transported power is increased by the factor α at given V with very little change in the transport lattice. Only the half period length has been decreased by the small factor $\alpha^{-1/4}$. The big change is that the depressed tune σ is decreased by the factor $\alpha^{-3/4}$. A discussion of tune limits is given below.

There are many possible linac configurations for a given value of q; the low cost optimum is found by LIACEP. One attractive possibility (not optimal) is found by simply applying the transformation [Eq. (27)] to a known configuration with q = 1, raising its charge to $q = \alpha$ and eliminating the high voltage portion of the linac so that the final kinetic energy is unchanged. This procedure is expected to yield incremental cost savings for the main portion of the linac of ~ 28% for each doubling of q, and in fact LIACEP verifies this approximate cost scale. This cost savings does not include the first 50 MV or the final

transport and focus lines. The total cost of these sectors will, in fact, increase with higher charge state so that an optimum charge state can be established.

At low voltage (V < 50 MV) the current that can be conveniently transported with superconducting quadrupoles is low, and the use of electrostatic quadrupoles is preferred. Unfortunately, the scale law for increased charge state is not attractive for this form of transport. It is found that the electric line charge density per meter is limited by the value[16]

$$\lambda \lesssim \left(.6 \frac{\mu C}{m}\right) \frac{\phi(a)}{50\ kV} \quad , \tag{28}$$

where we assume $\sigma_0 = 90°$, $\sigma \ll \sigma_0$, and $\eta = 1/2$. Hence electric current increases only as $q^{1/2}$, and we are led to consider a large number of beamlets of small radius, which are merged for the magnetic transport lattice.

In the early work on transport limits, Maschke adopted the values $\sigma_0 = 90°$ and $\sigma/\sigma_0 = 1/\sqrt{2}$. In fact, it is not immediately apparent from Eqs. (10)-(12) that a higher allowed value of σ_0 and lower allowed σ will result in lowered accelerator costs since the beam radius is also increased as the current increases. However, from Eq. (13), the current density increases as $\sigma_0^{2/3}$ for $\sigma \ll \sigma_0$ and for fixed α, η, and B. Hence, it is good to raise σ_0 as high as possible. A lower allowed value for σ permits either a lower normalized emittance or increased charge to mass ratio.

Since the work of Maschke there have been several developments in the understanding of tune limits, which now stand at the values $\sigma_0 \lesssim 80°$, $\sigma/\sigma_0 \gtrsim .1$; a brief summary of part of this work is given here:

a. Analytical calculations[49] showed that the Kapchinskij-Vladimirskij (K-V) distribution of transverse phase space variables is unstable in stop bands depending on σ and σ_0. Perturbations of order n in the radial coordinate are potentially unstable for $\sigma_0 > 180°/n$. Simulation studies[49,50] supported this point by demonstrating the onset of the third order and second order (envelope) modes with characteristic phase space distortions. To stabilize these modes the conditions $\sigma_0 \leq 60°$, $\sigma \geq 24°$ were adopted for driver studies during the period 1981-84.

b. Simulation studies performed with realistic (non K-V) distributions [by I. Haber and C. Celata], have shown little evidence of unstable mode growth for $\sigma/\sigma_0 > .1$ and $\sigma_0 < 80°$. The principal diagnostic is the growth of transverse emittance. This empirical result may be the consequence of the detuning effect of the slightly rounded charge profile of the non-KV distributions, which could damp modes higher than n = 2 (the envelope equations and modes are nearly independent of distribution details).

c. Recent simulation work[47] has considered the effects of both images and higher order focal multipoles, which are always present to some degree. For large amplitude oscillations of the beam's centroid, the image forces are found to drive a coherent internal sextupole mode, resulting in emittance growth for $\sigma/\sigma_0 < .1$ and moderate values of σ_0 (60°-72°). This effect can be largely cancelled by the addition of dodecapole elements of appropriate magnitude.

d. High current transport experiments performed at LBL with a coasting 160 kV C^+_s beam focussed by an electrostatic FODO lattice yield the result[51] that for $\sigma_0 < 88°$ no current loss or emittance growth could be detected for values of σ/σ_0 as low as 0.1. A phenomenological rule for stability is (M. Tiefenback):

$$\omega_p \leq \frac{1}{3}\omega_L \ , \tag{29}$$

where ω_p is the plasma frequency within the pulse and

$$\omega_L = \frac{2\pi\sigma_0 V}{2L} \tag{30}$$

is the lattice frequency. This condition may be written

$$\sigma_0^2 - \sigma^2 < (85°)^2 \ . \tag{31}$$

A plot of results from this experiment is given in Fig. (8) along with the stability boundaries predicted for the envelope mode. A non-zero value of source emittance prevents experimental conclusions being made for very low tune values ($\sigma < 8°$ at $\sigma_0 = 60°$). Above σ_0 of 90°, instability is observed and this region is therefore not of interest for practical high-current linac design.

B. Strategy for Introduction of HIF

The projected cost of a heavy ion linear induction accelerator for inertial fusion has decreased substantially with the prospect of higher charge state ion sources, higher undepressed tunes and lower depressed tunes. Indeed, if these prospects continue to be substantiated in the laboratory, induction linear accelerators using heavy ions may become economically competitive with lasers for driving inertial fusion

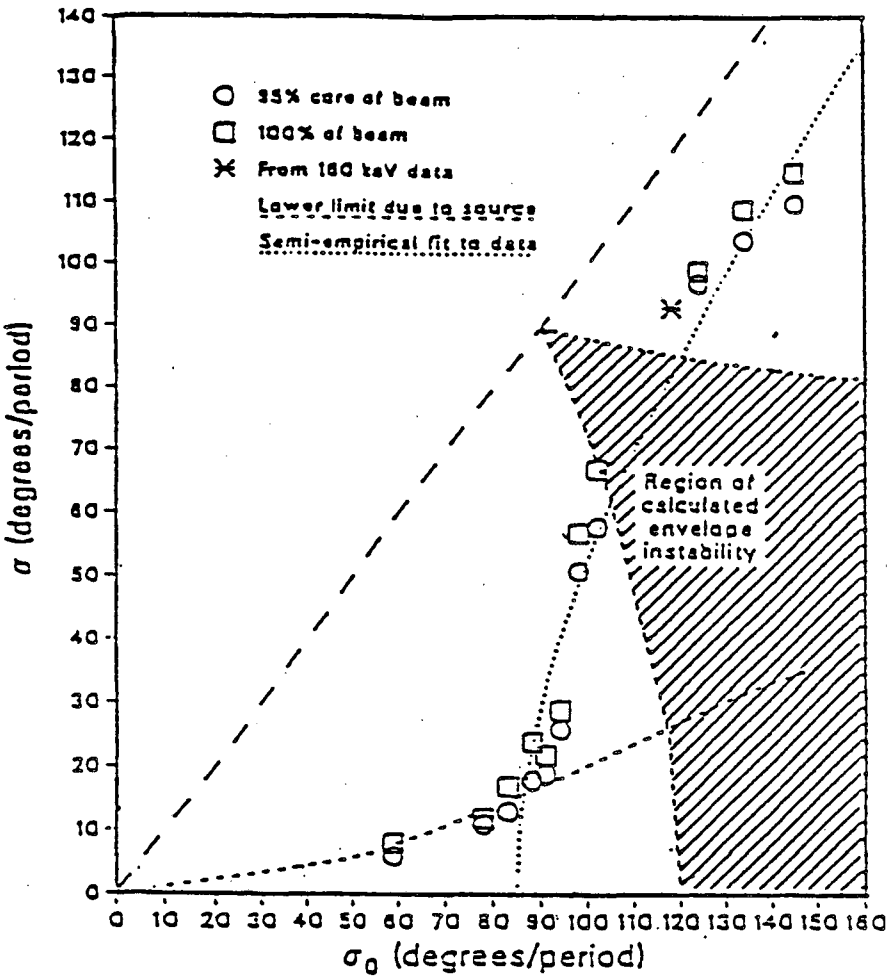

Fig. 8. The experimental limits on beam stability in terms of the undepressed tune (σ_0) and depressed tune (σ). Zones of predicted and observed instability are depicted in the (σ, σ_0) plane. The cross hatched area corresponds to the unstable envelope mode predicted for the KV distribution. Data points (except for those on the lower broken line) indicate the onset of emittance growth or disruption as σ_0 is increased, with the phenomenological fit $\omega_p = \omega_L/3$ given by the dotted line. The zone below the lower broken line is inaccessible due to the non-zero emittance of the SBTE pulse (courtesy of M. Tiefenback).

reactions on a single pulse basis, as well as an inertial fusion electric power plant.

A Single Pulse Test Facility (otherwise called a Target Physics Demonstration Facility)[52] is the next step in the development and demonstration of the U.S. Inertial Confinement Fusion Program supported by the DoE Defense Programs. This facility, with driver pulse energy between 1 and 10 MJ, will be capable of both military and civilian applications experiments, in addition to target physics studies. Because of the higher efficiency of coupling of the beam energy to a target by heavy ions relative to short wavelength photons, if a heavy ion driver were selected, it might require as little as one-half the output energy on target as a laser.

The energy output of a given induction linac can be substantially increased by multiple pulsing, which has been demonstrated in the laboratory, where a sequence of pulses about 10 to 20 microseconds apart are produced with acceptable wave form in a scale demonstration. Thus, a heavy ion induction linac driver can double its output energy on target (at the cost of lowering the accelerator efficiency) by double pulsing, for only the incremental cost of the additional stored energy, fast pulsers to reset the cores between pulses, and the installation of beam delay lines between the final beam compression and bunching region and the target chamber. Since accelerator efficiency is not an issue in the early part of an ICF development scenario, a heavy ion 1 MJ induction linac can be used as a driver for the Single Pulse Test Facility (SPTF) to, for example, demonstrate target gain, and perhaps produce a target yield of about 40 MJ. This accelerator can be upgraded

to a driver output of 2 MJ by double pulsing or 4 MJ by quadruple pulsing (which may produce a target yield as high as 150 MJ).

The pulse repetition frequency of the accelerator can be increased to 1 Hz, and a second target chamber can be built. This facility, which can be operated in parallel with the existing Single Pulse Test Facility using the same accelerator, can be used as an Engineering Test Facility (ETF) for evaluating materials, civilian reactor concepts, and components, as well as perform other missions requiring a fusion environment. This Engineering Test Facility is capable of a fusion power of 150 MW, and will require the mass production of targets as well as a target injection system and a heat removal system for about 200 MW.

For a modest additional cost, the accelerator can be upgraded to a pulse repetition frequency of 3 Hz, and a third target chamber can be built, based on the results from the SPTF and the ETF. This target chamber, which can operate in parallel with the SPTF and the ETF if desired, will be integrated into a complete, scaled, engineered electric production plant for the net production of electricity from inertial fusion. This facility, called the Experimental Power Reactor (EPR), will produce 300 MW of fusion power with a net electric power to grid of 30 Mw_e if it is operating in parallel with the ETF, and 450 MW of fusion power with 120 MW_e net electric power if it is operating as a stand-alone machine.

The evaluation of the HIF facilities using the above strategy is given in Table VII, using 6.7 GeV, mass 200, charge state +3 ions, where the normalized emittance is 4 μm-radians. The gains are based on the Lindl-Mark curve[34] for single-shell targets, using the lower bound target spot radius determined at 1 MJ of driver output energy.

Table VII. Evolution of Facilities by Multiple Pulsing an Induction Linac Driver Producing 1 MJ per Pulse in a HIF Development Scenario.

Energy Output MJ	Pulses	Repetition Rate hertz	Fusion Power MW
1	1	< 1	< 40
2	2	< 1	< 150
2	2	1	150
2	2	3	450

Increasing the driver output energy to 2 MJ will require that the target spot radius be increased by about 50%, which can be done in the final optics.

The HIF development scenario given above may result in an attractive buy-in price for the driver portion of the Single Pulse Test Facility. Since this would be a first-of-a kind device, we are unable to readily estimate its cost in 1985 dollars. However, percentage incremental costs for its extension as an ETF and EPR driver have been made. The upgrade incremental cost of the accelerator for use in an ETF is about 32%. This machine would simultaneously drive the SPTF and ETF. For an additional 3.5% incremental cost, which covers the upgrade to a higher rep rate, the HIF community will possess an accelerator that can simultaneously drive SPTF, ETF, and an EPR. Separate accelerators for the three facilities would cost 275% of the combined use machine. It must be pointed out here that the additional transport lines and final focus magnets for these facilities will add a substantial and unknown cost, estimated roughly at 10% of the total for each facility.

Other accelerator upgrade scenarios can be constructed to implement the HIF development scenarios using multiple pulsing and taking advantage of the small cost of increasing the pulse repetition frequency of induction linear accelerators. The options, coupled with physical separability of the driver from the fusion reaction chamber intrinsic to inertial fusion could make possible a cost effective path to the operation of an Experimental Power Reactor based on inertial fusion using induction linacs as part of a heavy ion driver.

VII. CONCLUSIONS

Recent advances in the technology and experimental results on key transport physics issues result in increased prospects for signficantly reducing the projected cost of a linear induction accelerator using heavy ions as a driver for inertial fusion. These advances include a source that produces high currents with a substantial percentage of ions at a selected charge state greater than +1 and low emittance. The stability of a heavy ion beam transported with a high undepressed tune and a low depressed tune has been demonstrated in the Single Beam Transport Experiment. The acceleration of several parallel beamlets sharing a single core has been demonstrated[54] in the Multiple Beam Experiment. Multiple pulsing of cores has been demonstrated. Other important issues such as combining beamlets in a matching section at the transition from electrostatic focussing to magnetic focussing, bending of space charge dominated beams, drift compression, and final focus physics, can be investigated in the proposed scaled driver experiment ILSE[54] for a relatively small cost.

An intrinsic advantage of inertial fusion, that the driver is separable from the fusion reaction chamber, can be utilized to operate several fusion reaction chambers from a common driver. This is possible by switching the driver beam to the various chambers in the time interval between beam pulses by using simple switching magnets. Because the incremental cost of increasing the accelerator pulse repetition frequency is small, and because the output heavy ion beam energy from a linear induction accelerator can be multiplied by multiple pulsing at a small fraction of the initial cost, a cost effective scenario for the development of inertial fusion is possible. This scenario would use a

single heavy ion linear induction accelerator as a driver, with several upgrades, for a Single Pulse Test Facility to be used for target physics studies, as well as civilian and military applications. An Engineering Test Facility would test materials and inertial fusion reactor concepts and subsystems, and an Inertial Fusion Experimental Power Reactor addresses issues in an integrated inertial fusion reactor facility with a net production of electrical power. These facilities would be constructed in series, but operated in parallel.

The use of energetic heavy ion beams from linear induction accelerators is a cost-effective, minimum risk way to proceed in the shortest time to commercial power from inertial fusion. A strategy includes the use of heavy ions from an induction linac for all the intermediate facilities between the current Nova/PBFA class of machines and a commercial fusion power plant.

VIII. REFERENCES

1. A.W. Maschke, "Relativistic Heavy Ions for Fusion Applications," IEEE Trans. Nucl. Sci., NS-22, No. 3, p. 1825 (June, 1975).

2. ERDA Summer Study of Heavy Ions for Inertial Fusion, (R.O. Bangerter, W. B. Herrmannsfeldt, D. L. Judd, and L. Smith, editors), Lawrence Berkeley Laboratory Report LBL-5543, Berkeley, CA (December, 1976).

3. Proceedings of the Heavy Ion Workshop Held at Brookhaven National Laboratory-1977, (L.W. Smith, editor), Brookhaven National Laboratory Report BNL-50769, Upton, NY (1978).

4. B. Badger, et al., "HIBALL-II, An Improved Conceptual Heavy Ion Beam Driven Fusion Reactor Study," Kernforschungszentrum Karlsruhe Report KFK 3840, Karlsruhe, FRG (July, 1985).

5. T. Katayama, A. Itano, A. Noda, M. Takanaka, S. Yamada, and Y. Hirao, "Design Study of a Heavy Ion Fusion Driver, HIBLIC-I," Laser and Particle Beams, 3, Part 1, p. 9 (February, 1985); also, Proc. 1984 INS Int. Symp. Heavy Ion Accelerators and Their Application to Inertial Fusion, p. 192, Institute for Nuclear Study, Tokyo, Japan (1984).

6. C.L. Olson, "Final Tranport in Gas and Plasma," Proc. of the Heavy Ion Workshop, p. 403, Lawrence Berkeley Laboratory Report LBL-10301, Berkeley, CA (September, 1980).

7. J.H. Pitts and I. Maya, "The Cascade Inertia-Confinement-Fusion Power Plant," Proc. 11th Symp. on Fusion Engineering, p. 130, Austin, TX (Nov. 1985).

8. J.A. Blink, W.J. Hogan, J. Hovingh, W.R. Meir, and J.H. Pitts, "The High-Yield Lithium-Injected Fusion-Energy (HYLIFE) Reactor," Lawrence Livermore National Laboratory Report UCRL-53559, Livermore, CA (1985).

9. P. Stroud, "Streaming Modes in Final Beam Transport for Heavy Ion Beam Fusion," Laser and Particle Beams, 4, Part 2, p. 261 (May, 1986).

10. J. D. Lawson, The Physics of Charged-Particle Beams, Clarendon Press, Oxford (1977).

11. The Multiple Beam Experiment (MBE-16) Conceptual Design as of June 1984 (D. L. Judd, editor), Lawrence Berkeley Laboratory Report PUB-5123, Berkeley, CA (October, 1984).

12. L. J. Laslett, "Concerning an A-G Transport System with σ_0 = 60 Degrees," Lawrence Berkeley Laboratory Informal Note HI-FAN-56, Berkeley, CA (October, 1978).

13. G. Lambertson, L.J. Laslett, L. Smith, "Transport of Intense Ion Beams," IEEE Trans. Nucl. Sci., NS-24, No. 3, p. 993 (June, 1977); also, LBL-5552.

14. E.D. Courant and H.S. Snyder, "Theory of the Alternating-Gradient Synchrotron," Annals of Physics, 3, p. 1, Academic Press, NY (1958).

15. I.M. Kapchinskij and V.V. Vladimirskij, "Limitations of Proton Beam Current in a Strong Focusing Linear Accelerator Associated with the Beam Space Charge," Proc. Int. Conf. on High Energy Accelerators, p. 274 CERN (1959).

16. E.P. Lee, T.J. Fessenden, and L.J. Laslett, "Transportable Charge in a Periodic Alternating Gradient System," IEEE Trans. Nucl. Sci., NS-26, No. 5, p. 2489 (October, 1985); also, LBL-19560.

17. E.D. Courant, "Power Transport in Quadrupole or Solenoid-Focussing Systems," Proc. ERDA Summer Study of Heavy Ions for Inertial Fusion, p. 72, Lawrence Berkeley Laboratory Report LBL-5543, Berkeley CA (December, 1976).

18. E. P. Lee, "Transport of Intense Ion Beams," Proc. Second Int. Conf. on Charged Particle Optics, Albuquerque, NM, May 19-23, 1986 (to be published); also, Lawrence Berkeley Laboratory Report LBL-21559, Berkeley, CA (June, 1986).

19. R. L. Martin, "Emittance Limitations in Heavy Ion Fusion," Nucl. Instruments and Methods, 187, p. 271 (1981).

20. D. Keefe, "Research on High Beam-Current Accelerators," Particle Accelerators, 11, p. 187 (1981).

21. S. Humphries, Jr., Principles of Charged Particle Acceleration, Wiley Interscience, NY (1986).

22. Proceedings of the Heavy Ion Workshop Held at Argonne National Laboratory-1978 (R. C. Arnold, editor), Argonne National Laboratory Report ANL-79-41, Argonne, IL (1979).

23. Proceedings of the Heavy Ion Workshop Held at Claremont Hotel-1979 (W. B. Herrmannsfeldt, editor), Lawrence Berkeley Laboratory Report LBL-10301, Berkeley, CA (September, 1980).

24. T. J. Fessenden, "Induction Linacs for Heavy Ion Fusion Research," Proc. 1984 Linear Accelerator Conference, p. 485, Seeheim/Darmstadt, FRG (September, 1984); also, Lawrence Berkeley Laboratory Report LBL-17788, Berkeley, CA (May, 1984).

25. Proceedings of the Symposium on Accelerator Aspects of Heavy Ion Fusion Held at Gesellschaft für Schwerionenforschung-1982, (D. Böhne, editor), Gesellschaft für Schwerionenforschung Report GSI-82-8, Darmstadt, FRG (1982).

26. Proceedings of the 1984 INS International Symposium on Heavy Ion Accelerators and Their Application to Inertial Fusion, (Y. Hirao, T. Katayama and N. Tokuda, editors), Institute for Nuclear Study, University of Tokyo, Tokyo, Japan (1984).

27. A. Faltens, E. Hoyer, D. Keefe, and L. J. Laslett, "Design/Cost Study of an Induction Linac for Heavy Ions for Pellet Fusion," IEEE Trans. Nucl. Sci., NS-26, 3, p. 3106 (1979); also, LBL-8357.

28. A. Faltens, E. Hoyer, D. Keefe, and L. J. Laslett, "Status Report on the Lawrence Berkeley Laboratory Heavy Ion Fusion Program, Part I, A Design and Cost Procedure for Heavy-Ion Induction Linacs," Proceedings of the Heavy Ion Fusion Workshop held at Argonne National Laboratory-1978, (R. C. Arnold, editor), Argonne National Laboratory Report-79-41, Argonne, IL, p. 31 (1979).

29. A. Faltens, E. Hoyer and D. Keefe, "A 3 Megajoule Heavy Ion Fusion Driver," Proc. 4th Int. Top. Conf. on High-Power Electron and Ion-Beam Research and Technology, Palaiseau, France (1981); also LBL-12409.

30. W.H. Kohl, Handbook of Materials and Techniques for Vacuum Devices, p. 596, Reinhold Publishing Co., New York (1967).

31. A. Faltens and S.S. Rosenblum, "Investigation of Re-X Glass Ceramic for Accelerator Insulating Columns," IEEE Trans. Nucl. Sci., NS-32, No. 5, p. 3131 (October 1985); also, LBL-19526.

32. L. M. Waganer, D. S. Zuckerman, K. W. Billman, and W. W. Saylor, "Critical System Issues for an HIF Reactor," Proc. 11 Symp. on Fusion Engineering, Austin, TX (November, 1985).

33. M. J. Monsler, J. Hovingh, D. L. Cook, T. G. Frank, and G. A. Moses, "An Overview of Inertial Fusion Reactor Design," Nuclear Technology/Fusion, I, p. 302 (July 1981).

34. J. D. Lindl and J. W-K. Mark, "Recent Livermore Estimates on the Energy Gain of Cryogenic Single-Shell Ion Beam Targets," Lasers and Particle Beams, 3, Part 1, p. 37 (1985).

35. R.O. Bangerter, J. W-K. Mark, and A. R. Thiessen, "Heavy Ion Inertial Fusion: Initial Survey of Target Gain Versus Ion Beam Parameters," Phys. Lett. A, 88, p. 225 (1982).

36. J. Hovingh, V. O. Brady, A. Faltens, E. Hoyer, and E. P. Lee, "Cost/Performance Analysis of an Induction Linac Drive System for Inertial Fusion," Proc. 11th Symp. on Fusion Engr., p. 975, Austin, TX (Nov. 1985); LBL-20613.

37. L. M. Waganer, D. E. Driemeyer and D. S. Zuckerman, "Survey of System Options for Heavy Ion Fusion," Proceedings of the International Symposium on Heavy Ion Fusion, (to be published), Washington, D.C. (May, 1986).

38. D. S. Zuckerman, D. E. Driemeyer, L. M. Waganer, J. Hovingh, E. P. Lee, and K. W. Billman, "Performance and Cost Modeling of a Linac-Driver HIF Power Plant," Proceedings of the International Symposium on Heavy Ion Fusion, (to be published), Washington, D.C. (May, 1986).

39. D. E. Driemeyer, L. M. Waganer, and D. S. Zuckerman, "Influence of System Optimization Considerations on LIA Driver," Proceedings of the International Symposium on Heavy Ion Fusion, (to be published), Washington, D.C. (May, 1986).

40. I. Brown, "An Intense Metal Ion Beam Source for HIF," Heavy Ion Fusion, AIP Conference Proceedings, 152, p. 207, American Institute of Physics, New York (1986), (M. Reiser, T. Godlove, eds.); also LBL 21593.

41. E.P. Lee, "Accelerator and Final Focus Model for an Induction Linac Based HIF System Study," Heavy Ion Fusion, AIP Conference Proceedings, 152, p. 461, American Institute of Physics, New York (1986), (M. Reiser, T. Godlove, eds.); also LBL-21346.

42. A. Faltens and D. Keefe, "Quasi-Static Drift-Tube Accelerating Structure for Low Speed Heavy Ions," Particle Accelerators, 8, p. 245 (1978); also LBL-7200.

43. J. Hovingh, V.O. Brady, A. Faltens, D. Keefe, and E.P. Lee, "The Cost of Induction Linac Drivers for Inertial Fusion for Various Target Yields," Heavy Ion Fusion, AIP Conference Proceedings, 152, p. 474, American Institute of Physics, New York (1986), (M. Reiser, T. Godlove, eds.); also LBL-21350.

44. A. Faltens and L.J. Laslett, Lawrence Berkeley Laboratory, private communication (May, 1986).

45. J. Hovingh, V.O. Brady, A. Faltens, and E.P. Lee, "A Comparison of the Design and Costs of Induction Linac Drivers for Inertial Fusion Using Ions of Mass 133 and 200," Fusion Technology (to be published); also LBL-21826.

46. J. Hovingh, V.O. Brady, A. Faltens, and E.P. Lee, "A Comparison of the Design and Costs of Induction Linac Drivers for Inertial Fusion Using Ions of Differing Mass," Trans. Am. Nucl. Soc., 52, 289 (1986); also LBL-20979.

47. C.M. Celata, I. Haber, L.J. Laslett, L. Smith, and M.G. Tiefenback, "The Effects of Induced Charge at Boundaries on Transverse Dynamics of a Space-Charge-Dominated Beam," IEEE Trans. Nucl. Sci., NS-32, No. 5, 2480 (1985); also LBL-19485.

48. D.S. Zuckerman, D.E. Driemeyer and L.M. Waganer, "A Systems Performance and Cost Model for Heavy Ion Fusion," Trans Am. Nucl. Soc., 52, p. 295 (1986).

49. I. Hofmann, L. J. Laslett, L. Smith and I. Haber, "Stability of the Kapchinskij-Vladimirskij (K-V) Distribution in Long Periodic Transport Systems," Particle Accelerators, 13, p. 145 (1983).

50. I. Hofmann, "Emittance Growth of Ion Beams with Space Charge," Nucl. Instr. and Methods., 187 P. 281 (1981).

51. M.G. Tiefenback and D. Keefe, "Measurements of Stability LImits for a Space-Charge-Dominated Ion Beam in a Long A.G. Transport Channel," IEEE Trans. Nucl. Sci., NS-32, No. 5, 2483 (1985); also LBL-19647.

52. J. Blink. "Inertial Confinement Fusion Development Options: Facility Characteristics and Schedule from a Reactor Physics Viewpoint," Fusion Technology, 9, p. 381 (May, 1986).

53. T. Fessenden, D.L. Judd, D. Keefe, C. Kim, L.J. Laslett, L. Smith, and A.I. Warwick, "Preliminary Results from MBE-4: A Four Beam Induction Linac for Heavy Ion Fusion Research," Heavy Ion Fusion, AIP Conference Proceedings, 152, p. 145, American Institute of Physics, New York (1986), (M. Reiser, T. Godlove, eds.).

54. T.J. Fessenden et al., "Preliminary Design of a 10 MeV Ion Accelerator for HIF Research," Lawrence Berkeley Laboratory report LBL-21194 (1986).

IX. FIGURE CAPTIONS

Fig. 1. Schematic of current concept for a 3.3 MJ driver that uses ions with A = 200, q = 3.

Fig. 2. Transverse motion of a particle in an alternating gradient focussing lattice. A lattice period corresponds to a focussing lens, a drift, a defocussing lens, and another drift (FODO). The definition of phase advance per period of the quasi-sinusoidal motion is shown for cases in which space-charge effects are negligible (top, σ_0), and strong (bottom, σ).

Fig. 3. The accelerator core module features the insulator internal to the cores.

Fig. 4. Accelerator Parameter Space as a Function of Target Yield for a Range of Target Spot Radii for Ion Mass 200 amu.

Fig. 5. Normalized Cost of Accelerator Per Unit Fusion Power as a Function of Target Yield for Several Fusion Power Outputs and a Range of Target Spot Radii for Ion Mass 200 amu, charge state +1.

Fig. 6. Distribution of the accelerator costs (1979 dollars per volt) as a function of ion kinetic energy for a 300 MJ target yield producing a fusion power of 3000 MW. The transition ion energy for 64 beamlets to 16 beamlets is 400 MeV (133 MV). Above the transition ion energy the depressed tune is 7.5°.

Fig. 7. Cumulative distribution of the accelerator costs (1979 dollars) as a function of ion kinetic energy for a 300 MJ target yield producing a fusion power of 3000 MW. The transition ion kinetic energy for 64 beamlets to 16 beamlets is 400 MeV.

Fig. 8. The experimental limits on beam stability in terms of the undepressed time (σ_0) and depressed tune (σ). Zones of predicted and observed instability are depicted in the (σ,σ_0) plane. The cross hatched area corresponds to the unstable envelope mode predicted for the KV distribution. Data points (except for those on the lower broken line) indicate the onset of emittance growth or disruption as σ_0 is increased, with the phenomenological fit $\omega_p = \omega_L/3$ given by the dotted line. The zone below the lower broken line is inaccessible due to the non-zero emittance of the SBTE pulse (courtesy of M. Tiefenback).

X. ACKNOWLEDGEMENT

This work was supported by the Office of Program Analysis, U.S. Department of energy, under Contract No. DE-AC03-76SF00098.

LAWRENCE BERKELEY LABORATORY
TECHNICAL INFORMATION DEPARTMENT
UNIVERSITY OF CALIFORNIA
BERKELEY, CALIFORNIA 94720